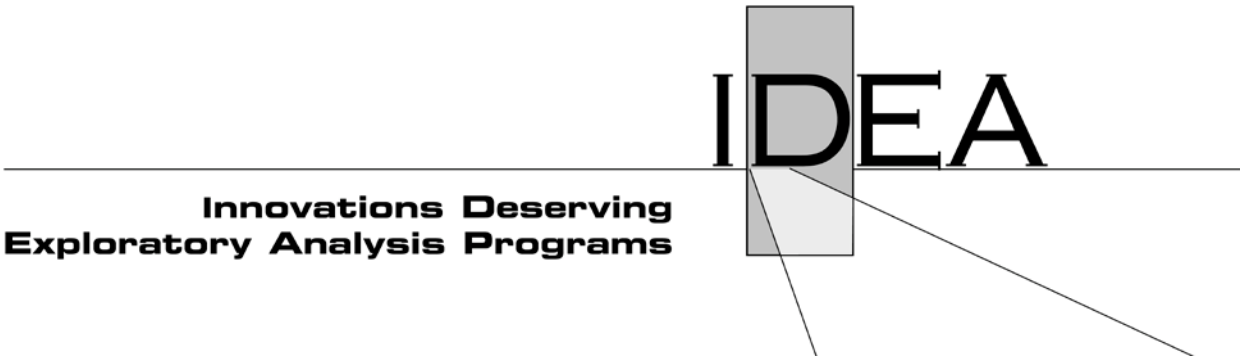

NCHRP IDEA Program

Graphene Nanoplatelet (GNP) Reinforced Asphalt Mixtures: A Novel Multifunctional Pavement Material

Final Report for
NCHRP IDEA Project 173

Prepared by:
Jialiang Le, Mihai Marasteanu, Mugurel Turos
University of Minnesota

January 2016

TRB TRANSPORTATION RESEARCH BOARD
The National Academies of
SCIENCES · ENGINEERING · MEDICINE

Innovations Deserving Exploratory Analysis (IDEA) Programs Managed by the Transportation Research Board

This IDEA project was funded by the NCHRP IDEA Program.

The TRB currently manages the following three IDEA programs:

- The NCHRP IDEA Program, which focuses on advances in the design, construction, and maintenance of highway systems, is funded by American Association of State Highway and Transportation Officials (AASHTO) as part of the National Cooperative Highway Research Program (NCHRP).
- The Safety IDEA Program currently focuses on innovative approaches for improving railroad safety or performance. The program is currently funded by the Federal Railroad Administration (FRA). The program was previously jointly funded by the Federal Motor Carrier Safety Administration (FMCSA) and the FRA.
- The Transit IDEA Program, which supports development and testing of innovative concepts and methods for advancing transit practice, is funded by the Federal Transit Administration (FTA) as part of the Transit Cooperative Research Program (TCRP).

Management of the three IDEA programs is coordinated to promote the development and testing of innovative concepts, methods, and technologies.

For information on the IDEA programs, check the IDEA website (www.trb.org/idea). For questions, contact the IDEA programs office by telephone at (202) 334-3310.

IDEA Programs
Transportation Research Board
500 Fifth Street, NW
Washington, DC 20001

Graphene Nanoplatelet (GNP) Reinforced Asphalt Mixtures:

A Novel Multifunctional Pavement Material

IDEA Program Final Report

NCHRP IDEA 173

Prepared for the IDEA Program

Transportation Research Board

The National Academies

Jialiang Le
Mihai Marasteanu
Mugurel Turos

University of Minnesota

April 2016

TABLE OF CONTENTS

LIST OF TABLES

LIST OF FIGURES

ACKNOWLEDGMENTS

The authors would like to thank Georgene Geary, Georgia Department of Transportation, for her contribution as the IDEA advisor for this project.

The authors would like to acknowledge the assistance provided by Shongtao Dai and Eddie Johnson, Minnesota Department of Transportation, for the experimental investigation of the rutting performance of GNP-reinforced asphalt mixtures.

Special recognition goes to Dr. Inam Jawed for his support and guidance during the entire duration of this project.

EXECUTIVE SUMMARY

This project investigates the mechanical and compaction properties of graphene nanoplatelet (GNP) reinforced asphalt binders and mixtures, which are regarded as a potential candidate for the new generation of multi-functional asphalt pavement materials. The report first summarizes the current knowledge of the application of nanotechnology to asphalt materials. Meanwhile, it also provides an overview of some basic features of GNP materials with their applications to civil engineering, which motivate the investigation of their potential application to pavement materials.

In the subsequent sections, the report presents a series of experiments evaluating the mechanical properties of GNP-reinforced asphalt binders and mixtures that include a detailed method for material preparation and a quantitative analysis of the effect of GNP on the mechanical properties of asphalt binders and mixtures. It has been found that the GNP can be mixed with asphalt binders without major dispersion problems. This study involves binder and mixture specimens prepared with different amounts and types of GNP. For each type of mix designs, three types of mechanical tests are performed: (i) complex modulus test of the GNP-reinforced binders at room temperature; (ii) indirect tension creep and strength tests of the GNP-reinforced binders and mixtures measuring the creep, relaxation, and strength properties; and (iii) fracture test of the GNP-reinforced mixtures at low temperature measuring the fracture energy. These tests show that the addition of GNPs can greatly enhance the flexural strength of asphalt binders at low temperatures and moderately improve the creep stiffness, but has no adverse effects on relaxation properties. It is also observed that, compared with conventional asphalt mixtures, GNP-reinforced asphalt mixture specimens exhibit an improved strength and, in some cases, an increase in fracture energy. However, with the current mixing procedure, GNP addition does not improve the electrical conductivity of the asphalt materials.

In addition to mechanical properties, the compaction process of GNP-reinforced asphalt mixtures is investigated, which involves the following aspects: (i) the compaction effort in terms of number of gyrations for a target air void content; (ii) the air void content that can be achieved for a given compaction effort; and (iii) the compaction temperature for a given compaction effort and target air void content. It has been experimentally observed that the addition of GNPs can significantly reduce the number of gyrations needed to compact the mixtures to a target air void content. This reduction ranges from 15% to 40% for different mix designs. Furthermore, the GNP also allows successful compaction at a lower temperature.

The results of this project indicate that the GNP-reinforced asphalt binders and mixtures exhibit several improved mechanical and compaction properties. These improvements are strongly dependent on the mix design as well as the compaction process. Overall, this new type of asphalt materials has a potential for improving the performance as well as the cost-effectiveness of asphalt pavements.

CHAPTER 1

IDEA PRODUCT, CONCEPT, AND INNOVATION

About 90% of the highways and roads in the United States are constructed by using asphalt mixtures. There has been a sustained amount of effort devoted to improving the performance of asphalt pavements. A major part of these efforts was focused on the development of new asphalt-based pavement materials to achieve better mechanical properties. Recently, there has been an emerging interest in applying nanotechnology to asphalt pavement materials (*1*, *2*), and it was postulated that nanotechnology can potentially play a major role in the improved use of existing and available materials in pavements and in the material processing to improve the sustainability and resilience of pavements. In recent years, attempts have been made to incorporate carbon nanotubes (CNTs) into asphalt binders and mixtures, and it was found that the dispersion of CNTs in asphalt binders represents a major challenge (*2*). Some particular types of asphalt emulsions have to be used to achieve a good dispersion. With the relatively high material cost, the application of CNTs in asphalt pavements is rather limited.

This study explores the application of graphene nanoplatelet (GNP) to asphalt binders and mixtures, with specific attention on the evaluation of the mechanical and compaction. GNP is made from exfoliated graphene (Figure 1.1), which has been shown to possess superior mechanical and electron transport properties (*3*–*6*). The aspect ratio of GNP is significantly lower than that of CNT, which makes it easier to disperse. It is expected that the addition of GNPs into asphalt materials would improve various material properties, which are closely related to the performance of asphalt pavements. Meanwhile, it is known that the GNP materials also have lubricant effect (*7*), which may enhance the compaction process of the mixtures. Moreover, the cost of GNP is comparable to some commonly used polymer modifiers, such as styrene butadiene styrene (SBS), which makes it suitable for asphalt applications. Therefore, the GNP-reinforced asphalt binders and mixtures could be considered as potential candidates for the next generation of asphalt pavement materials, which would lead to a considerable reduction in the construction cost and improvement in durability of asphalt roads.

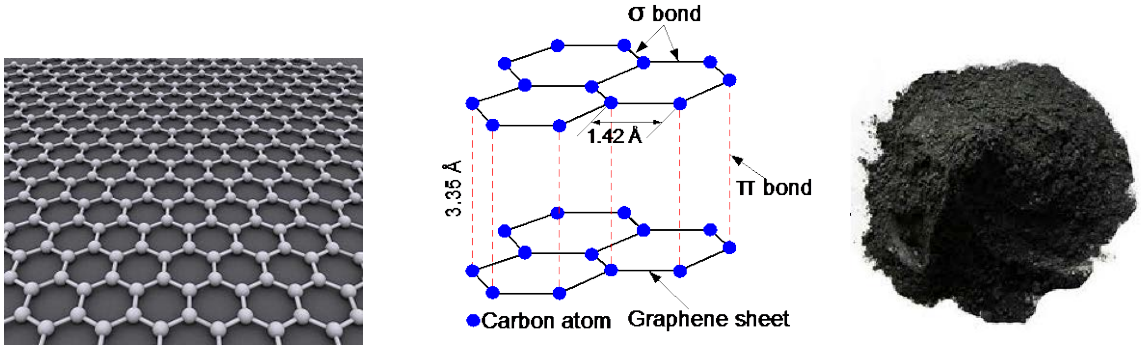

(a) (b) (c)

FIGURE 1.1: Graphene nanoplatelet (GNP): (a) graphene sheet, (b) atomic structure of GNP, and (c) as received GNP materials.

This research is designed to test the abovementioned hypotheses through a comprehensive evaluation of the mechanical and compaction properties of GNP-reinforced asphalt binders and mixtures. Chapter 2 briefly summarizes the application of nanotechnology to asphalt materials. Chapter 3 provides the results of mechanical properties of GNP-reinforced asphalt binders, which include complex modulus, creep, and strength. Chapter 4 presents the investigation of compaction process of GNP-reinforced asphalt mixtures. Chapter 5 reviews the measured mechanical properties of GNP-reinforced asphalt mixtures. Chapter 6 discusses the effect of GNP on the electrical conductivity of asphalt binders. The conclusions and the plans for implementation of GNP-reinforced binders and mixtures are presented in Chapter 7.

CHAPTER 2

APPLICATIONS OF NANOTECHNOLOGY TO ASPHALT MATERIALS

In recent years, there has been an emerging interest in applying nanotechnology to asphalt pavement materials. It is believed that nanotechnology could potentially have a major contribution to the sustainability and resilience of the pavement. A nanoparticle is generally defined as a particle with its least dimension being less than 100 nanometers (*8*). Recent research has suggested that nanoclay, nanosilica, carbon nanotubes, and basalt fibers could lead to an improvement of the performance of the asphalt mixtures. This chapter presents a summary of the results of these studies, and it also provides an overview of some basic features of GNP and its recent applications to civil infrastructure materials.

2.1 NANOCLAY

Nanoclays are nanoparticles of layered mineral silicates. While being a naturally occurring inorganic material, nanoclay can be altered to make it compatible with organic monomers and polymers and has a layer thickness on the order of one nanometer (*8, 9*). Compared with polymer-modified binder, nanoclays are relatively inexpensive since they are naturally occurring (*10*). Not only are nanoclays a more cost-efficient option, they also have favorable mechanical properties such as their nanoscopic size and surface area, which have shown tendencies for increasing the stiffness of asphalt binders (*11*).

Extensive research has been devoted toward the use of nanoclays to reinforce asphalt binders. Although some types of nanoclay did not affect the stiffness or viscosity of the bitumen, other types of nanoclay showed encouraging results (*5*). Upon testing stiffness and tensile strength, tensile modulus, flexural strength, and modulus thermal stability, it was found that, compared with unmodified bitumen, the elastic modulus increased for the nanoclay-modified bitumen while the dissipation of mechanical energy was lower (*8, 12*). Bentonite clay (BT) and organically modified bentonite (OBT) were also used to reinforce asphalt binders in pavement mixtures. While analyzed under shearing stresses and sonication, the modified asphalts ultimately had a higher rutting resistance, which could improve the low temperature rheological properties of asphalt (*5, 13*).

To gain a better understanding into the benefits of nanoclay-modified binders, the nanostructure and microstructure as well as the mechanical behavior of asphalt clay nanocomposites has been investigated. Many atomic force microscopy (AFM) techniques were employed including tapping mode imaging, force spectroscopy, and nanoindentation as well as X-ray diffraction (XRD) experiments. These techniques indicated that nanoclay had an exfoliated structure with enhanced adhesive forces (*14*). Specific nanoscale properties such as the state of dispersion and the exfoliation of the nanoclay binders have also been analyzed using techniques such as scanning electron microscopy (SEM) and XRD approaches (*11*). Fourier transform infrared spectroscopy (FTIR) has also been employed to evaluate the interactions between nanoclay and asphalt (*15*). The investigation of the nanoscale properties of the binders indicated that the improvement of the stiffness and hardness of the asphalt would depend on the temperature and percentage of nanoclay. These improvements appeared to result from the network of exfoliated nanoclay layers and the aggregates (*14*). In general, the improvement of mechanical properties of the asphalt mixture can be better understood by the interactions of the aggregates and binders at a nanoscopic scale.

Recent studies with nanoclay-modified binders also showed an increase in the Superpave rutting factor and the rotational viscosity (RV) tests indicated a significant increase in viscosity. These results pointed toward nanoclay as an alternative to polymer-modified binders for more cost-efficient pavement solutions and maintenance (*11*). Meanwhile, dynamic mechanical analysis, flexural creep stiffness, and flexural tests on nanoclay-modified binders indicated that the temperature susceptibility and complex modulus increase, while the phase angle decreases (*15*). Other laboratory methods including the surface free energy (SFE) and small angle X-ray diffraction (SAXD) techniques have been applied to nanoclay-modified asphalt mixtures to investigate the moisture susceptibility properties of nanoclay-modified asphalt binders (*10*). Among its other benefits, nanoclay has also been found to improve the aging resistance and storage-ability of asphalt mixtures (*8, 16*).

2.2 NANOSILICA

Silica is also an abundant compound that has applications outside of material science in areas such as medication and drug distribution (*8, 17*). Nanosilica has also been used to reinforce elastomers as a rheological solute (*8*). Similar to nanoclay, nanosilica is beneficial owing to its low production cost and high performance (*8*). Laboratory testing has found a slight decrease in viscosity values with the addition of nanosilica in asphalt. This indicates that the compaction temperatures would be lower or a lower energy of the construction process could be achieved (*8*). It was found that the

addition of nanosilica could enhance anti-aging, fatigue cracking and rutting resistance, and anti-stripping properties. Although beneficial in some aspects, the low temperature performance of nanosilica in asphalt binders was not remarkable. The stress relaxation capacity remained the same for nanosilica-modified asphalt binders and, in general, the low temperature properties of the asphalt binders were not greatly affected (*8, 18*).

Techniques used to analyze nanosilica-enhanced binders include morphological, rheological, and thermal analysis. Differential scanning calorimetry (DSC), thermogravimetric analysis (TGA), AFM, and FTIR were also used to quantify the effect of nanosilica as a binder modifier. The optimum content of the nanosilica modifier could be determined based primarily on the results from dynamic shear rheometer (DSR) asphalt fatigue and rutting tests (*19*). Moisture susceptibility, resilient modulus, and dynamic creep tests were also employed to evaluate the performance of nanosilica particles added to polymer modified asphalt mixtures under different aging and moisture susceptibility conditions (*20*). SEM was used to analyze how well the particle dispersed into the asphalt binder. It was found that nanosilica could reduce the susceptibility to moisture damage and increase the strength as well as enhance the fatigue and rutting resistance of asphalt binders (*20*). Additional laboratory tests include rotational viscosity (RV), bending beam rheometer (BBR), and flow number (FN) tests showing signs of an improved dynamic modulus, flow number, and improved rutting and fatigue performance (*20*). The results indicated that nanosilica produces beneficial results for asphalt pavement materials, but does not specifically improve these materials under low temperature conditions.

2.3 CARBON NANOTUBES

Carbon nanotubes (CNTs) are one-atom-thin sheets of graphite shaped into a hollow cylinder (*8*) (Figure 2.1). Their diameter is on the order of one nanometer and CNTs have superior mechanical properties with high tensile strength (*8*). Although there is less available literature for the use of CNTs to reinforce asphalt binders, improvements have been documented. Most prominently investigated in two forms, single and multi-wall nanotubes have been analyzed using atomic force microscopy. When adding CNTs to asphalt, an increase in adhesive forces has been noted as well as an increase in moisture susceptibility (*21*). The morphology of CNT-modified hot mix asphalt was also examined using scanning electron microscopy. The mechanical properties including resilient modulus, creep behavior, and fatigue performance indicated that CNTs could produce an improvement against fatigue and permanent deformation compared with conventional HMA (*22*).

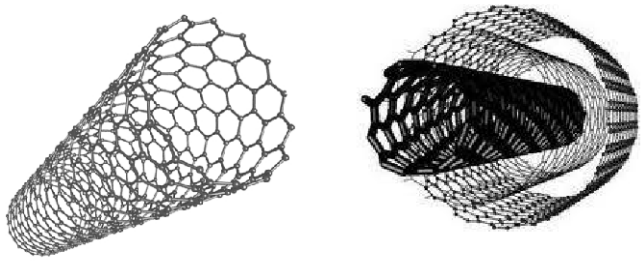

(a) (b)

FIGURE 2.1: Carbon nanotube (CNT) structures: (a) single-wall CNT and (b) multi-wall CNT.

Overall, previous research showed that CNTs could enhance the rutting resistance potential and the resistance to thermal cracking (*8*). However, the major challenge of the application of CNTs is the dispersion issue. It was found that good dispersion could be achieved by using some particular types of asphalt emulsions. Meanwhile, the relatively high material cost of CNTs also limits their applications in asphalt pavements.

2.4 BASALT FIBERS

Basalt fiber is a material made from fine fibers of basalt, resembling carbon fiber and fiberglass. It is highly resistant to alkaline and salt, creating potential use for concrete, bridge, and shoreline structures (*23*). Dynamic shear rheological tests and creep tests have indicated that basalt fibers could lead to an improvement in the performance of asphalt binders (*24*). Basalt fiber-reinforced asphalt mixtures have demonstrated a high absorption ratio, low water absorption ratio, and high tensile strength and temperature stability (*24*). Fatigue properties of asphalt mixtures under harsh environmental conditions, chloride penetration, freezing-thawing cycle, and their coupling effects were studied for basalt fiber-reinforced asphalt mixtures (*25*). The optimum dosage of basalt fiber was determined using the Marshall test and the results indicated that the tensile strength, the maximum curving tensile stress, the curving stiffness modulus, and fatigue

properties are influenced by the chloride erosion and freezing-thawing cycle (*26*). Therefore, low temperature fracture and fatigue properties of asphalt mixtures could be improved by adding moderate amounts of basalt fibers. The direct tension test results showed that the basalt fibers could improve the tensile strength of the asphalt binders (*26*). Experimental results also indicated a reduction in failure stiffness and an overall improved low temperature cracking resistance of asphalt concrete at low temperatures with basalt fiber reinforcement (*27*).

2.5 INTRODUCTION TO GRAPHENE NANOPLATELETS

Previous research efforts have demonstrated that nanotechnology provides a promising means of improving the properties of asphalt materials. Most existing studies have focused on the mechanical properties of modified asphalt at intermediate temperatures. Few studies have investigated the mechanical properties at low temperatures, which are crucial for asphalt pavements under harsh winter conditions. One of the major barriers of the application of advanced nano-materials to asphalt industry is the considerably high material cost. Therefore, the motivation of this study is to explore some cost-effective nano-material that is suitable for asphalt pavements and examine its effect on both the manufacturing process and the mechanical properties of asphalt binders and mixtures.

This study focuses on GNPs. The GNPs consist of stacks of graphene sheets that can be characterized as nano-discs with a diameter of sub-micrometer and a thickness on the order of a nanometer. A graphene sheet is a single layer of carbon atoms with a hexagonal arrangement. Graphene material exhibits superior mechanical and electron transport properties: the stiffness of graphene is on the order of 1 TPa, the strength of graphene is approximately 100 times that of steel, and the electric conductivity of graphene is higher than that of copper (*3–5*). Furthermore, it has been shown that graphene has an exceptional thermal stability up to at least 2600 K (*6*). The cost of GNP materials depends on its type and carbon purity. For large-scale applications, the material cost can be as low as $3–$4 per pound, which is significantly lower than the cost of multi-wall CNTs. It can be noted that the material cost of GNPs is comparable to some existing asphalt modifier such as the styrene butadiene styrene.

A series of studies has recently been performed on the application of GNPs in cement mortar (*28–30*). It was found that the addition of GNPs could effectively enhance the electrical conductivity of cement mortar (*28*). This makes cement a damage-sensing material in which the relative increase in electrical resistance can be explicitly related to the damage level of the material. Meanwhile, it was also demonstrated that the GNPs would reduce the critical pore diameter of the cement mortar and thus improve the resistance of the cement mortar to water permeability, chloride diffusion, and chloride migration. This has a significant impact on the durability of the material (*29*). Experiments also showed that the addition of GNPs would lead to an increase in elastic modulus and tensile strength of cement mortar (*30*).

These studies have demonstrated the potential benefits of the application of GNPs to civil engineering materials. With the relatively low material cost GNPs could be suitable for large-scale infrastructure applications. These merits of GNP materials stimulate the proposed research, which explores the potential application of GNPs in asphalt materials with an aim of improving the overall performance of our asphalt pavements.

CHAPTER 3

MECHANICAL PROPERTIES OF GNP-REINFORCED ASPHALT BINDERS

This chapter presents a summary of the experimental work on the mechanical properties of GNP-reinforced asphalt binders. The experiments involve two types of binders and three types of GNP materials. For each GNP material, two different amounts of GNP addition are considered. The present experimental program consists of the complex shear modulus test, flexural creep test, and the flexural strength test.

3.1 SAMPLE PREPARATION

In this study, two types of asphalt binder were used for testing, an unmodified asphalt binder PG 52-34 and a SBS-modified asphalt binder PG 64-34. The base binder PG 52-34 was chosen for the purpose of exploring the potential of replacing SBS by GNP. The base binder PG 64-34 was chosen to examine whether the GNP could further enhance the performance of SBS-modified binder and mixture. Both binders were obtained from Minnesota Department of Transportation (MnDOT), and were manufactured by Flint Hills Resources. For the GNP materials, three types of GNP manufactured by Asbury Graphite Mills were used in this study, as listed in Table 3.1.

TABLE 3.1 GNP materials

GNP type	Description	Carbon Content	Surface Area (m^2/g)	Cost ($/lb)
M750	Graphite nano-flake powder	96.22%	13	2.95
M850	Graphite nano-flake powder	99.54%	13	3.53
4827	Surface enhanced synthetic graphene material	99.66%	250	4.14

Batches of 100 g binder and the GNP materials were heated for 30 minutes in an oven at 150°C for the PG 52-34 binder and at 160°C for the PG 64-34 binder and then stirred together on a hot plate for 10 minutes with a glass rod until a homogeneous mix was observed. In total, three types of GNP materials (i.e., M750, M850, and 4827) were used and, for each GNP type, two different mixing amounts (3% and 6% by weight of the binder) were considered in this study. These two amounts were chosen based on the initial calculation of the required GNP amount for improving the electrical conductivity using the percolation theory, which will be discussed in Section 6.2). Table 3.2 presents the seven different combinations of binder and GNP that were made for each type of binder. During the mixing, we did not observe any potential clustering of the GNP, which is one of the main advantages of using GNP over the conventional CNTs.

TABLE 3.2 Combinations of asphalt binders and GNPs

	GNP Addition						
Binder	None	3% M850	6% M850	3% M750	6% M750	3% 4827	6% 4827
PG 64-34	X	X	X	X	X	X	X
PG 52-34	X	X	X	X	X	X	X

Each blend was short-term aged using a rolling thin film oven (RTFO) according to the AASHTO standard method T240 (*31*). This method provides the information on the change in binder properties during conventional hot mixing at the mixture production plant. The RTFO procedure also improves the blend homogenization. After using RTFO for short-term aging, a pressurized aging vessel (PAV) [AASHTO standard method R28-12 (*32*)] was used to accelerate the aging of the mix in order to simulate the in-service oxidative aging in the field for an asphalt pavement during 5–7 years of service. The aged binders can then be used to obtain the low and intermediate temperature properties of asphalt binders for specification purposes. When the aging procedure was completed, the blend was degassed using a vacuum oven, and then stored in small cans and reheated just one time and stirred before preparing the DSR and BBR test samples.

3.2 COMPLEX SHEAR MODULUS TEST

A DSR AR 2000, manufactured by TA Instruments, was used for the complex shear modulus test. A frequency sweep procedure based on the AASHTO standard method T315-12 (*33*) was performed at temperatures ranging from 4°C to 70°C and frequencies between 1 and 100 rad/s. The measured data were used to generate master curves of the norm of the complex modulus $|G^*|$ and phase angle δ for both RTFO and PAV aging conditions.

Figure 3.1 shows the measured complex shear modulus and phase angle of plain asphalt binders and the GNP-reinforced asphalt binders. The complex shear modulus and phase angle represent two essential viscoelastic properties of the binders at moderate and high temperatures. It can be seen that both the complex shear modulus and phase angle do not change significantly when GNP materials are added to the binders.

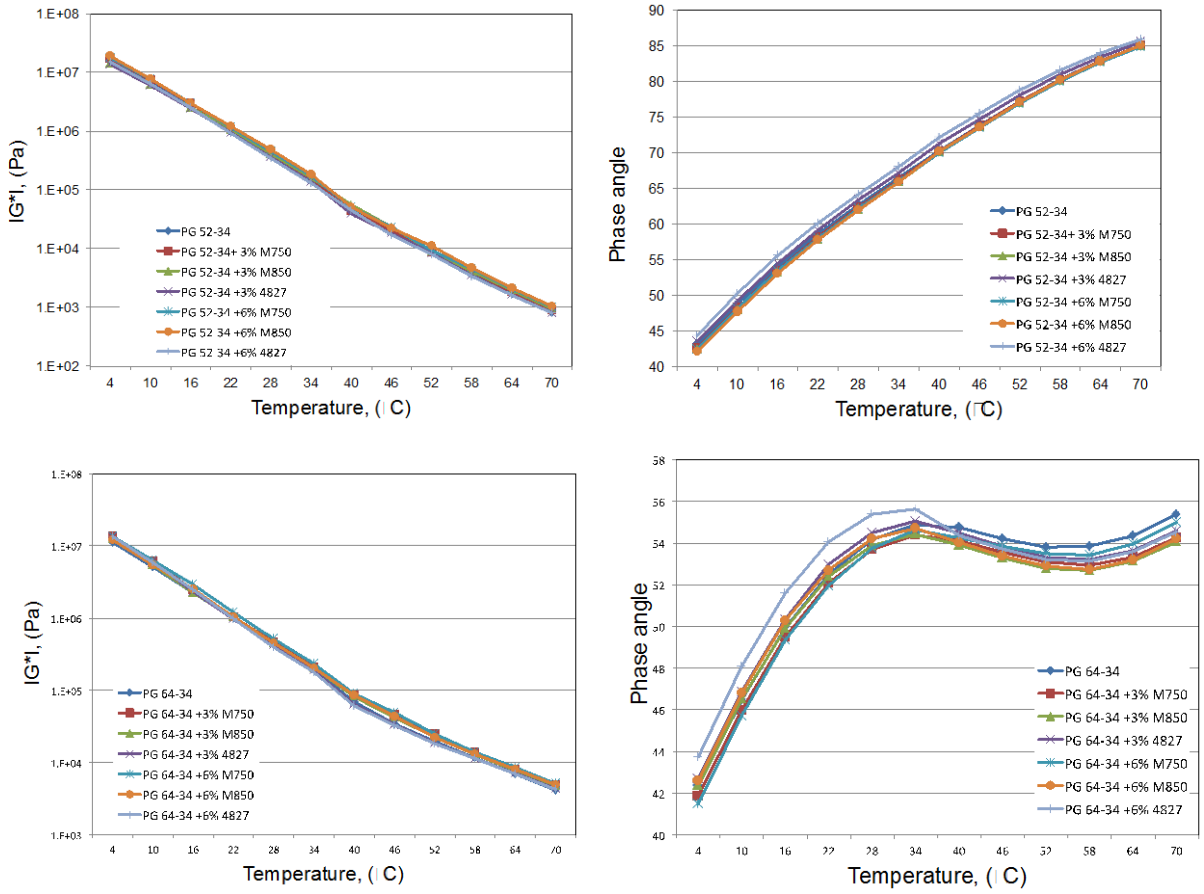

FIGURE 3.1: Measured complex shear modulus and phase angle of GNP-reinforced asphalt binders.

3.3 CREEP STIFFNESS TEST

A BBR, made by Cannon Instruments, was used to measure the creep stiffness. The testing procedure is in accordance with the AASHTO standard method T313-12 (*34*). The specimen has a size of 127 mm (length) × 6.35 mm (depth) × 12.7 mm (width). Three replicates were tested for each PAV blend in potassium acetate. Both the creep stiffness and the *m*-value (the slope of stiffness-time curve in the log-log scale) were obtained at two temperatures, PG+4°C and PG−2°C for the 3% GNP modified binder, and at PG−2°C for the 6% GNP modified binder, and compared between blends.

Figures 3.2 and 3.3 show the comparison of the creep stiffness (at 60 s) of plain asphalt binders and the GNP-modified asphalt binders. Creep stiffness represents the inverse of creep compliance, a fundamental property of viscoelastic materials. It has been found that the increase in creep stiffness is limited to 5%–15%. Comparing Figure 3.2 with Figure 3.3, it can be observed that a lager dose of GNPs leads to a slightly higher creep stiffness. Meanwhile, the slope (at 60 s) of the stiffness-time curve (in log-log space), usually referred to as the *m*-value, is seen to change

minimally. This indicates that the addition of GNPs does not significantly change the relaxation property of the material. It is worthwhile to mention that the measured results on creep stiffness and *m*-value are subjected to a considerable degree of variability. Such variability could be reduced through a better mixing procedure, such as the use of high-shear mixer.

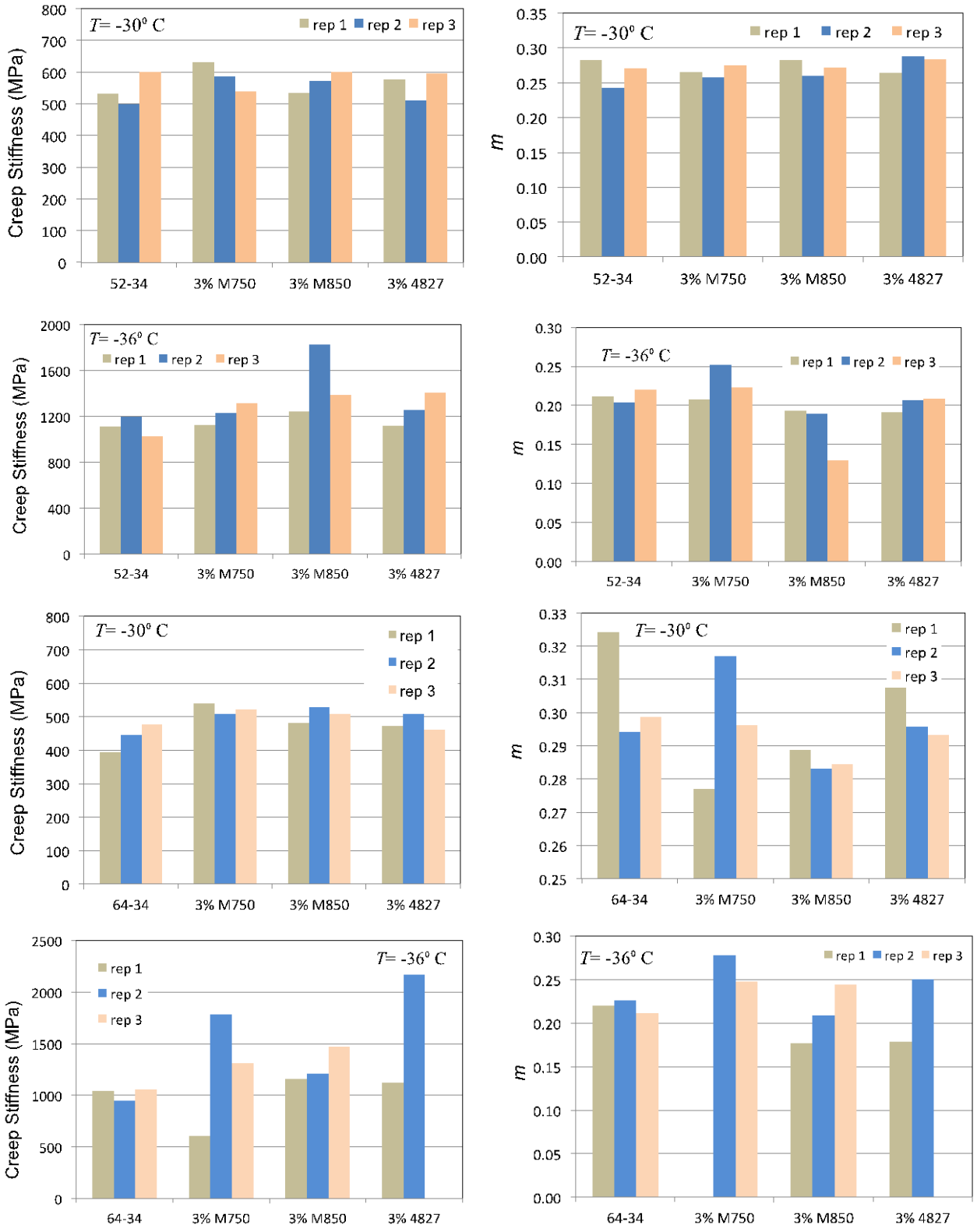

FIGURE 3.2: Measured creep stiffness and *m*-value of GNP-reinforced asphalt binders with 3% GNP addition.

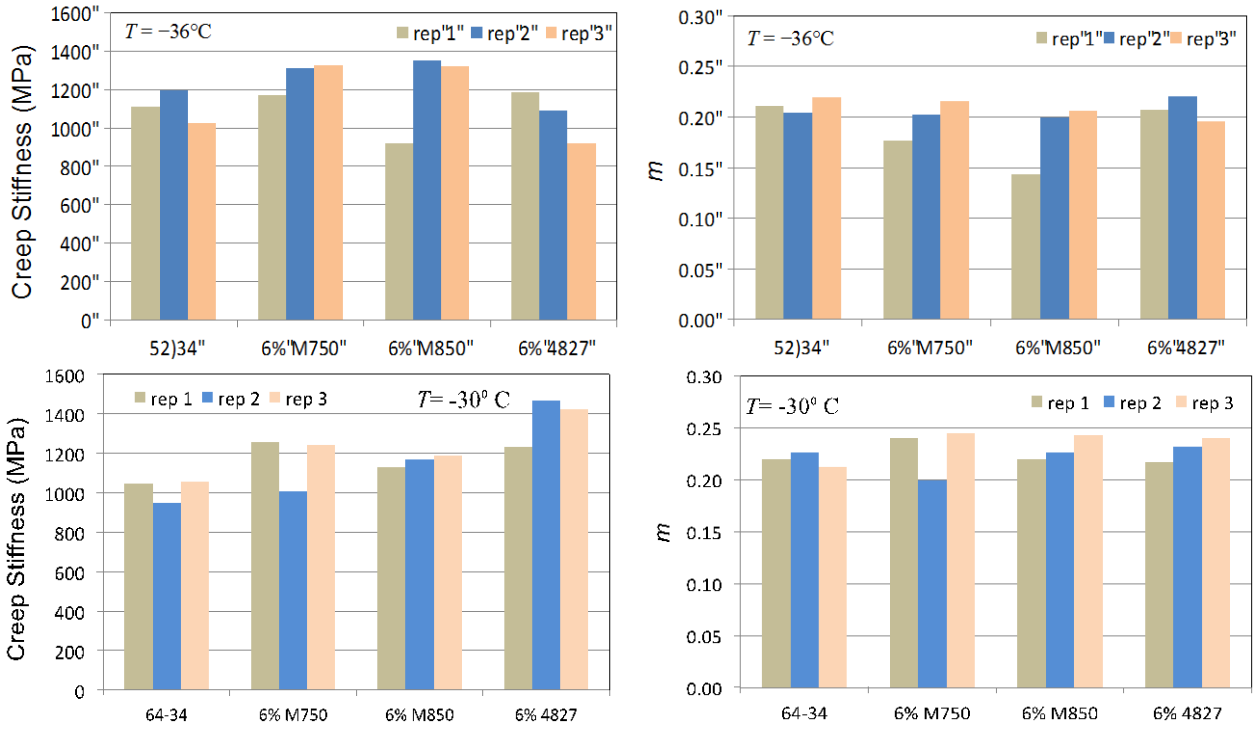

FIGURE 3.3: Measured creep stiffness and *m*-value of GNP-reinforced asphalt binders with 6% GNP addition.

3.4 FLEXURAL STRENGTH TEST

A modified BBR, with a proportional valve that offers a complex control of the pressure in the air bearing system, and a 44 N load cell, made by Cannon Instruments Company, called BBR-Pro, was utilized to perform the strength test. Specific software was used to control the loading pattern, to perform the compliance correction, and to record the load and the deflection every time unit (0.25 s). Figure 3.4 shows the modified BBR test apparatus.

In this case, instead of running a creep test using a constant load, a strength test was performed: the load was increased at a constant rate until the beam failed. The BBR nominal strength ($\sigma_N = P_{max}/bD$, where P_{max} = peak load, b= beam width, D = beam depth) and corresponding strain ε_N at the bottom of the thin beam were recorded for each beam. Tests were run in potassium acetate at two temperatures, PG+4°C and PG−2°C, for the 3% GNP-modified binder, and at PG−2°C for the 6% GNP-modified binder.

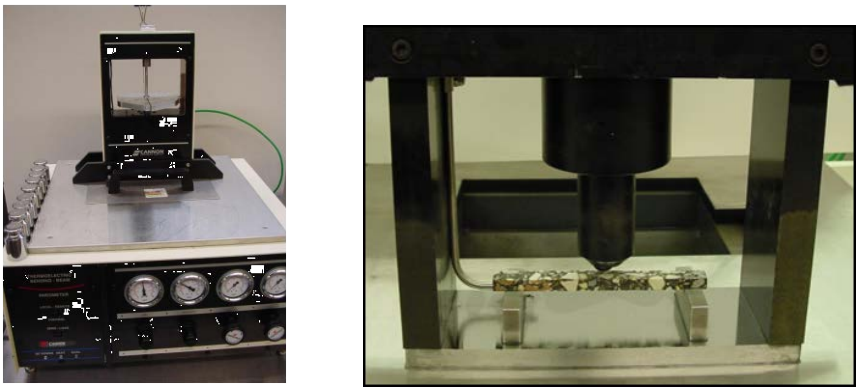

FIGURE 3.4: (a) BBR strength test set-up and (b) close-view of BBR test specimen.

Figure 3.5 shows the comparison of the measured flexural strength of plain asphalt binders and the GNP-modified asphalt binders. It can be seen that the addition of all three types of GNP has a significant impact on the strength

properties of the binder PG 52-34. On average, addition of 3% of GNP M750 leads to an 80% strength increase, addition of 3% GNP M850 improves the strength by 1.5 times, and addition of 3% GNP 4827 improves the strength by 1.3 times. These are remarkable improvements that have not been observed with any other additives used in binder modification. Meanwhile, it can be observed that addition of a large amount of GNP material (6%) does not lead to a proportionally higher strength. This indicates that there is an optimum amount of GNP addition to the binders for strength enhancement. Based on the present experiments, it is seen that 3% GNP addition is more cost-effective than 6% GNP addition for improving the binder strength.

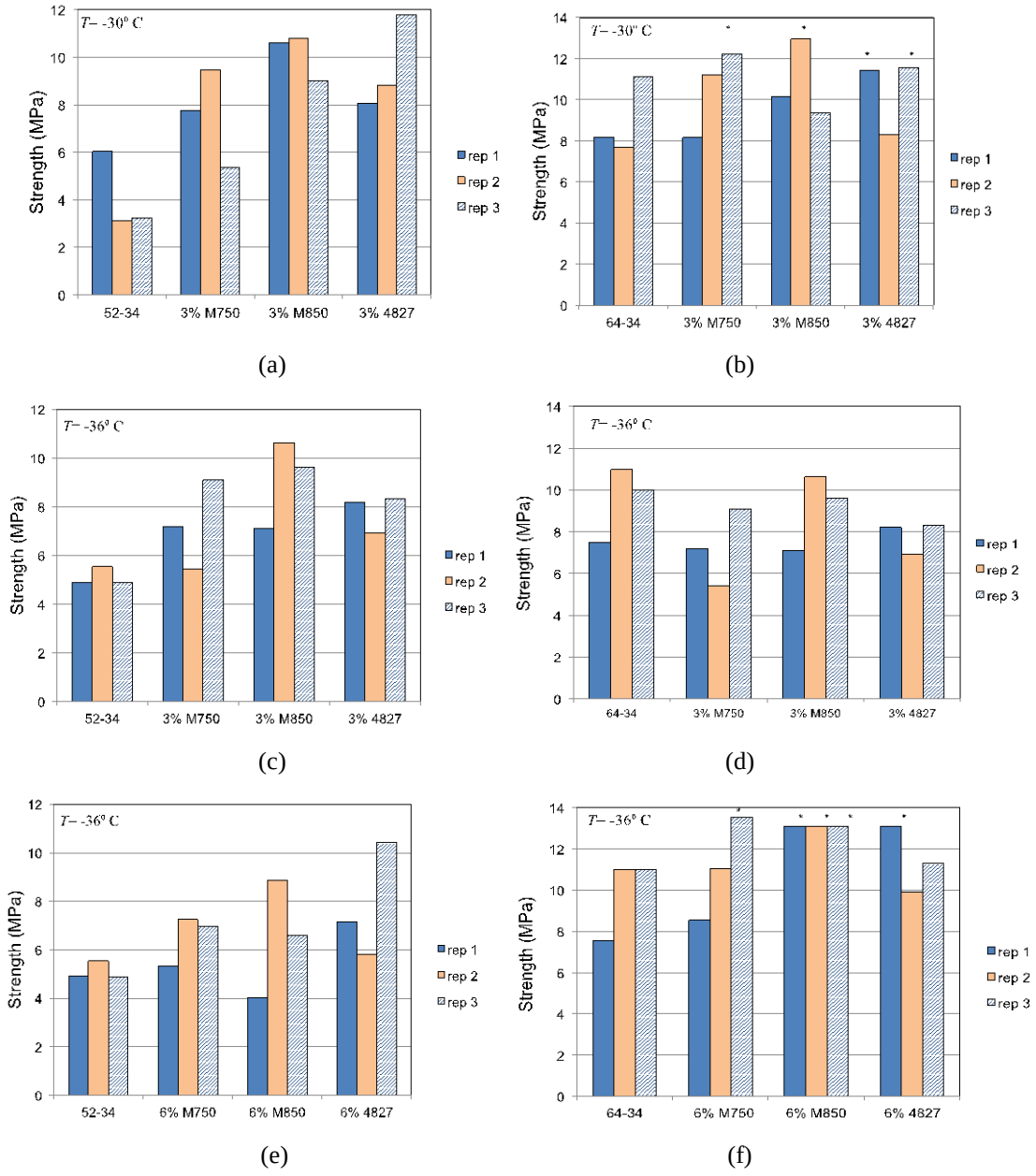

FIGURE 3.5: Measured flexural strength of GNP-reinforced asphalt binders.

The observed strength improvement for PG 52-34 is similar to the recently observed effect of GNP on the tensile strength of cement mortar (*30*). The strength improvement resulting from the addition of GNPs does not always increase with the addition amount. This could be because if a larger dose of GNPs is used the GNPs could potentially clump together even though the aspect ratio is low. The clumping hinders the effective dispersion of the GNPs into binders and thus causes less strength improvement. It is interesting to note that such a phenomenon has also been observed in the

application of CNTs in cement, where it was shown that as the CNT amount exceeds some value the improvement of strength of cement nearly vanishes because of the clumping issue (*35*).

In this set of experiments, we also observed improvements when the GNPs were added into the polymer-modified binder (PG 64-34). The starred bars indicate that the strength capacity of the material exceeded the testing equipment limits and the strength could be higher than the values plotted. As a result, we cannot determine the exact increase of strength for this case. Nevertheless, we can conclude that the strength is increasing by at least 60% for addition of 6% GNPs. By contrast, addition of 3% GNPs does not lead to a significant increase in strength of modified PG 64-34 binder at $T = -36°C$.

Figure 3.6 shows the comparison of typical measured stress-strain curves of PG 52-34 asphalt binder and 3% GNP-modified PG 52-34 asphalt binders at $T = -36°C$. It can be noted that the addition of GNPs does not change the elastic modulus; meanwhile the critical strain at which the material strength is reached also increases with the addition of GNPs. This indicates that the material can sustain a larger deformation before breaking under the load-control test. Similar trend is observed for GNP modified PG 64-34 binders.

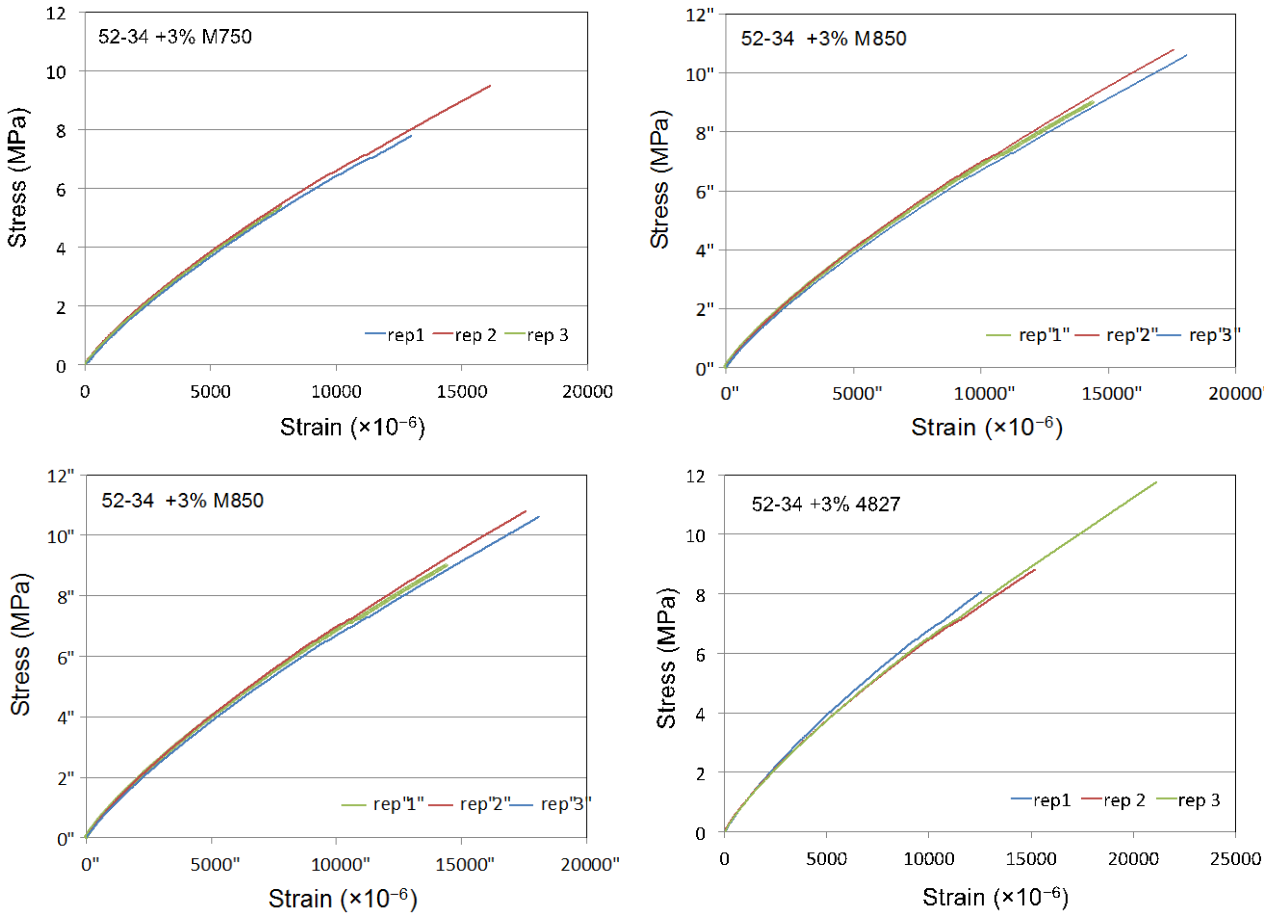

FIGURE 3.6: Measured stress-strain curves of 3% GNP-reinforced PG 52-34 asphalt binders ($T = -30°C$).

3.5 CONCLUSIONS

The present investigation of the mechanical properties of GNP-reinforced asphalt binders leads to the following observations:

1. The GNP does not have a significant effect on the complex modulus of the binder, which implies that the viscoelastic properties of the asphalt binders would be minimally affected by the GNP addition.
2. Compared with conventional polymer-modified and unmodified asphalt binders, the addition of GNPs can moderately increase the creep stiffness of the binder, but does not affect the "*m*" value, which is the slope of the

stiffness-time curve (in log-log space). This indicates that the GNP does not significantly affect the relaxation properties of the binder.

3. The GNP-reinforced asphalt binders exhibit superior flexural strength at low temperatures compared with the conventional asphalt binders. For both polymer-modified and unmodified asphalt binders, a moderate addition of GNPs; that is, 3% to 6% by weight of the binder can lead to as much as 130% increase in flexural strength. Such an increase has never been seen in polymer-modified asphalt binders. Meanwhile, it is observed that for unmodified binders the improvement of binder strength becomes less pronounced for large amount of GNP addition, which could be caused by the potential clumping of GNPs. On the contrary, for modified binders the high dose (6%) of GNPs is more effective than the low dose (3%).

CHAPTER 4

COMPACTION PROPERTIES OF GNP-REINFORCED ASPHALT MIXTURES

This chapter presents the experimental investigation of the compaction properties of GNP-reinforced asphalt mixtures, The essential parameters considered in this study include the required number of compaction gyrations, the compaction temperature, and the evolution of the air void content. In parallel with the compaction experiments, a set of rut experiments is also presented.

4.1 MATERIALS AND TESTING

The compaction experiments involve two mix designs provided by the MnDOT. All mixtures were prepared using Superpave mix design. The details of the mix design groups are as follows:

1. Mix design 1 is composed of 5.5% binder and four different types of aggregates, which include 67% Scandia BA 3/4 (gravel), 18% Kraemer 9/16 (limestone), 10% Kraemer 3/4 minus (limestone), and 5% Scandia screened sand (gravel). Two types of binders, unmodified PG 52-34 and SBS-modified asphalt cement PG 64-34, were considered for the mix design. The PG 52-34 binder was further modified with 3% 4827 GNP material, and the PG 64-34 binder was modified with 6% M850 GNP material.
2. Mix design 2 is composed of 5.7% unmodified binder PG 58-28 and three types of aggregates, which include 45% SSG sand, 25% Kraemer 3/8 minus (limestone), and 30% Kraemer 3/8 chip (limestone). For this mix design, the binder was modified by either 3% 4827 or 6% M850 GNP material.

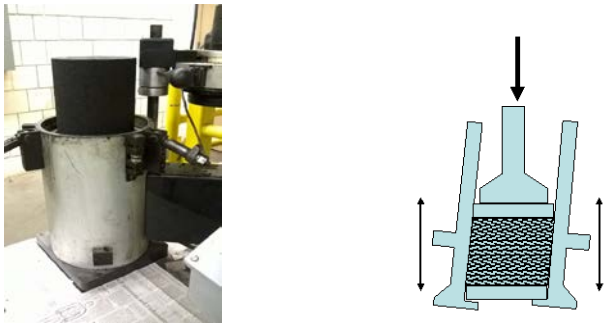

FIGURE 4.1: Sample compacted with the Brovold Gyratory Compactor.

The compaction test was performed using a Brovold Gyratory Compactor (Figure 4.1) at some prescribed temperatures. For each material type, three test replicates were used. The number of gyrations to reach a target air void content was recorded. The bulk specific gravity (GMB) and the maximum specific gravity (GMM) obtained for each set of binder and mixture were used to determine the compaction target height for the target air voids (*36*, *37*). Tables 4.1 and 4.2 present the compaction test matrices for mix design groups 1 and 2. A targeted air void content of 7% was chosen to match the air void value accepted and found in newly constructed pavements. It can be noted that for mix design group 2 the target air void content is 8%. This is because the experiments showed that the aggregate interlocking prevent compaction to a lower air void content for a reasonable number of gyrations.

TABLE 4.1 Test matrix for mix design group 1

Label	Binder	GNP Content (%, type)	Target Air Void Content	Compaction Temperature
X00-control	PG 52-34	None	7%	130°C
X00-control	PG 52-34	None	7%	90°C
X34	PG 52-34	3% 4827	7%	130°C
X34	PG 52-34	3% 4827	7%	90°C
A00-control	PG 64-34	None	7%	130°C
A00-control	PG 64-34	None	7%	90°C
A68	PG 64-34	6% M850	7%	130°C
A68	PG 64-34	6% M850	7%	90°C

TABLE 4.2 Test matrix for mix design group 2

Label	Binder	GNP Content (%, type)	Target Air Void Content	Compaction Temperature
Y00-control	PG 58-28	None	8%	130°C
Y00-control	PG 58-28	None	8%	100°C
Y34	PG 58-28	3% 4827	8%	130°C
Y34	PG 58-28	3% 4827	8%	100°C
Y68	PG 58-28	6% M850	8%	130°C
Y68	PG 58-28	6% M850	8%	100°C

4.2 RESULTS OF COMPACTION EXPERIMENTS

Tables 4.3 and 4.4 present the average numbers of gyrations N_{gyr} for the aforementioned two mix design groups. It is evident that the addition of GNP materials could lead to a reduction in the number of compaction gyrations at all compaction temperatures. This reduction is about 25% at T = 130°C, and the reduction is more significant at lower compaction temperatures, that is, T = 90°C and 100°C. By comparing the test results of mix design group 1 (X00-control, X34, and A00-control), it can be seen that the SBS-modified binder could also lead to a decrease in compaction gyration at T = 130°C, which is similar to the effect of GNPs. However, at T = 90°C the GNP-modified binder is much more effective than the SBS-modified binder in reducing the compaction effort. For mix design group 2, it is interesting to note that for the same base binder the two different types of GNP (4827 and M850) do not show a significant difference in compaction performance at T = 130°C, whereas this difference become much more substantial at T = 100°C. This clearly indicates that the effect of GNP on the compaction process is strongly temperature dependent. Such temperature dependence could be caused by the chemistry between the GNP and asphalt binder, which needs further investigations.

TABLE 4.3 Number of gyrations N_{gyr} of mix design group 1

	N_{qyr} for 7% Air Void Content	
Mix	T = 90°C	T = 130°C
X00-control	52	34
X34	30	26
A00-control	43	22
A68	32	17

TABLE 4.4 Number of gyrations N_{gyr} of mix design group 2

	N_{qyr} for 8% Air Void Content	
Mix	T = 100°C	T = 130°C
Y00-control	144	117
Y34	122	87
Y68	92	88

Meanwhile, it can also be observed that the decrease in compaction temperature leads to a higher demand in the number of gyration for all mix designs, which is a well-expected phenomenon. Nevertheless, it can be seen that for some GNP-reinforced asphalt mixtures (i.e., X34, Y68) the difference in the number of gyrations at different temperatures becomes significantly smaller. This indicates that the addition of GNPs would enable the compaction of the mixtures at a lower temperature, which could significantly reduce the energy input during the compaction process. Meanwhile, it should also be noted that this improvement depends on the mix design. For instance, for PG 52-34 binder the addition of GNP 4827 can effectively reduce the temperature effect on the compaction gyration, although this is not the case for PG 58-28 binder. Similarly, the addition of GNP M850 into modified PG 64-34 binder does not affect the temperature dependence of the compaction gyration while GNP M850 is seen to have a strong influence on such temperature dependence for PG 58-28 binder.

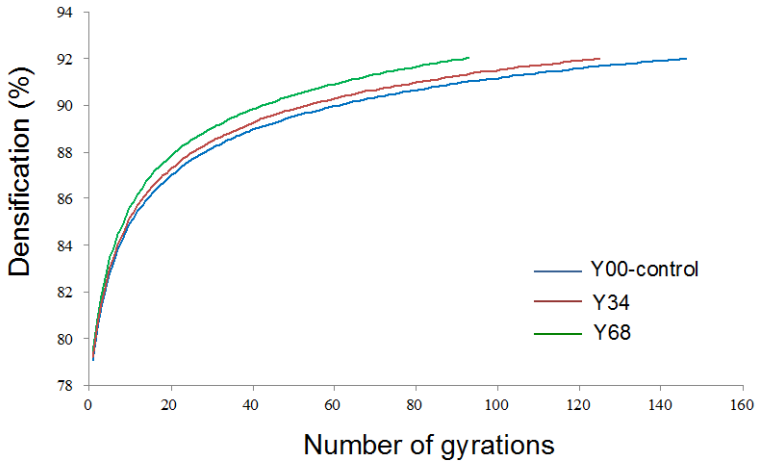

FIGURE 4.2: Typical measured compaction curve.

Figure 4.2 presents a set of compaction curves for mixes Y00-control, Y34, and Y68 at T = 100°C. It can be seen that for the densification ratio below 85% the compaction performances for these three mixes are similar. The main improvement occurs when compacting the specimens at the low air void content regime. The foregoing discussion focuses on the number of gyrations for a target air void content, and it is clear that the addition of GNPs could effectively reduce the compaction effort. On the other hand, if we fix the number of gyrations, the addition of GNPs would lead to a mixture with a lower air void content. For 100 gyrations, the mix Y00-control could reach a 90% densification ratio, whereas the mix Y68 could attain more than a 92% densification ratio. The reduction in the air void content has a significant implication on the durability of the pavements, such as lowering the risk of corrosion, reducing potential cracking during freeze-thaw cycles, and improving the fracture resistance of mixtures.

4.3 RUT EXPERIMENTS

One possible mechanism that is responsible for the observed reduction in compaction gyration for GNP-modified asphalt mixtures is the lubricating effect of the graphene material (*7*). This led us to investigate whether or not the addition of GNPs would have an adverse effect on the rutting performance. To this end, a set of rut experiments was performed for on several materials in mix design group 1 at the MnDOT. The air void content was controlled at 7%. The test materials include X00-control compacted at T = 130°C, X34 compacted at T = 90°C and T = 130°C, A00-control compacted at T = 130°C and A68 compacted at T = 90°C and T = 130°C. The rut experiments were carried out by using the Asphalt Pavement Analyzer, which is laboratory accelerated loading equipment for evaluating the rutting potential of HMA. The test temperature was set at 58°C, and the loading frequency was set to be 1Hz. Figure 4.3 shows the time evolution of the measured rut depth.

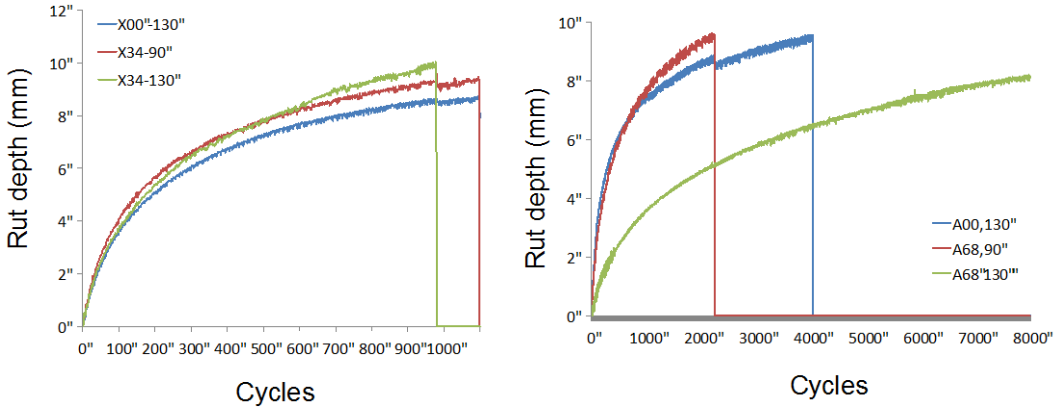

FIGURE 4.3: Measured rut performances of GNP-reinforced asphalt mixtures.

It can be observed that, for the mixture using the PG 52-34 binder (type “X”), the number of cycles to reach the rut depth maximum value is very low, and this number was almost the same for all the samples with and without GNP. Furthermore, the compaction temperature did not affect the results. Such a behavior can be attributed to the fact that the testing temperature that was higher than the average 7-day maximum pavement design temperature—the higher PG value. The performance of the type “A” mixture, tested at the same temperature, is different. The control A00-130 reaches the maximum measurable rut depth after 4,000 cycles, while the same mix design, using GNP added binder goes to 8,000 cycles. However, it is noted that the result for the mixture compacted at a much lower temperature T = 90°C is less favorable.

4.4 CONCLUSIONS

The compaction tests on GNP-reinforced asphalt mixtures show that the addition of GNPs into binders can significantly improve the compaction performance of the mixtures. For a target air void content, the GNP materials could lead to a 20%–40% reduction in the required number of compaction gyrations. Meanwhile, it is observed that for some mix designs the GNP could also reduce the temperature dependence of the compaction gyration, which allows engineers to produce warm asphalt mixtures. The measured compaction curves indicate that for a given number of compaction gyrations the addition of GNPs could effectively reduce the air void content of the final asphalt mixtures. This would improve the long-term durability of the pavements.

It can be noted that the improvement in compaction performance of the GNP-reinforced asphalt mixtures strongly depends on the type of the base binder. Meanwhile, the present results also imply that the chemistry between the binders and GNP that is responsible for the compaction process is also temperature dependent.

In parallel with the compaction tests, a set of rut experiments was performed and it demonstrated that the addition of GNPs improves the rut performance of the pavements at intermediate temperatures. Nevertheless, it can be observed that, if compacted at a lower temperature, the addition of GNPs could adversely affect the rut performance. Therefore, for each mix design there would be an optimal combination of the compaction temperature and the GNP addition and type to meet the specific requirements on construction cost, compaction performance, and rut performance.

CHAPTER 5

MECHANICAL PROPERTIES OF GNP-REINFORCED ASPHALT MIXTURES

This chapter presents the experimental investigation of the mechanical properties of GNP-reinforced asphalt mixtures, which involves two mix design groups. The experimental program consists of the indirect tension (IDT) creep test, IDT strength test, and Semi-Circular Beam (SCB) fracture test.

5.1 SAMPLE PREPARATION

Similar to the aforementioned compaction experiments, two mix design groups were considered for the experimental investigation of the mechanical properties of asphalt mixtures. The mix design details of these two groups follow the description in Section 4.1. Table 5.1 presents the different mix designs used in the present series of experiments. It is noted that for mix design group 2 the same mix design was used to produce the mixture specimens at two different compaction temperatures, through which we could investigate the effect of compaction temperature on the mechanical properties of the mixtures. For each mix design, six cylinders were compacted for each set of binder and GNP content.

TABLE 5.1 Test materials

	Compaction Temperature	Base Binder	No GNP Added	With 3% M850	With 6% M850	With 3% 4827	With 6% 4827
Mix design group 1	130°C	PG 64-34	A00	A38	A68	A34	A64
	130°C	PG 52-34	X00	X38	X68	X34	X64
Mix design group 2	130°C	PG 58-28	Y00-130	——	Y68-130	Y34-130	——
	100°C	PG 58-28	Y00-100	——	Y68-100	Y34-100	——

During the specimen preparation, the pans containing the aggregates, the one-gallon containers with the binders, and the cans with the right amount of GNP were heated in the oven for a total of 3 hours at 140°C for PG 52-34 and PG 58-38 binders and at 150°C for PG 64-34 binder. After 2 hours, GNPs were added to the binder and stirred for 15 minutes using a paint mixer and stored back in the oven for another hour. A Blakeslee B-20T mixer was used to mix the aggregates with the binder that has already been modified by the GNP. Prior to adding the GNP-modified binder mix to the aggregates, it was stirred again for another 5 minutes using the same paint mixer. After mixing, 7,000 g of the freshly made loose mix was put in the pan and the pan was covered and stored in the oven at 135°C for two more hours prior to compaction.

A Brovold Gyratory Compactor was used for the compaction. For mix design group 1, the compaction was performed at T = 130°C to achieve a 7% target air void content, whereas for mix design group 2 two compaction temperatures, T = 130°C and 100°C, were used with an 8% target air void content. The compacted samples were cut using a bridge saw with a 24-in. diamond blade. During the cutting process, water was used for cooling to prevent the damage of both the specimen and the cutting blade. Each cylinder was cut into four slices, in which the first layer with a thickness of 8 mm was discarded; the second and third layers with a 38-mm thickness were used for the IDT; the fourth layer with a 32-mm thickness was used for the SCB tests. To prepare the SCB specimens, the fourth slice was cut into two semi-cylindrical specimens along its diameter, and for each specimen a 15-mm notch was sawed at the center of the base.

5.2 IDT CREEP TEST

IDT creep tests were performed according to AASHTO Standard T322-07 (*38*). The tests were performed for a 1,000-s loading duration. The inverse of creep compliance, creep stiffness $S(t)$ was calculated at 60 s and 500 s for the present analysis. For mix design group 1, the creep tests were performed at T = −18°C and −28°C, while for mix design group 2 the tests were performed at T = −6°C and −18°C. The reason to choose T = −6°C is to investigate the effect of GNP on creep behavior at a higher temperature. For each mix, three tests were performed and the average value was presented in Figures 5.1 and 5.2.

It can be observed in Figure 5.1(a) that for mix design group 1 at T = −18°C for the GNP-reinforced mixtures with the polymer modified binder, the creep stiffness value after 60 s changes between −10% and +23% compared with A00 (mixture without GNP). After 500 s, the value varies between −17% and +17%. For mixtures with the unmodified binder, the stiffness largely decreases for the mixtures with added GNP. This decrease is up to 28% after 60 s and up to 33% after 500 s. At T = −28°C as shown in Figure 5.1(b) the results present a similar pattern, with an increase of up to 23% and a decrease up to 3% for the creep stiffness calculated for the GNP-reinforced mixtures with the polymer-modified binder. For GNP-reinforced mixtures with the unmodified binder, the creep stiffness is found to exhibit a slightly decrease.

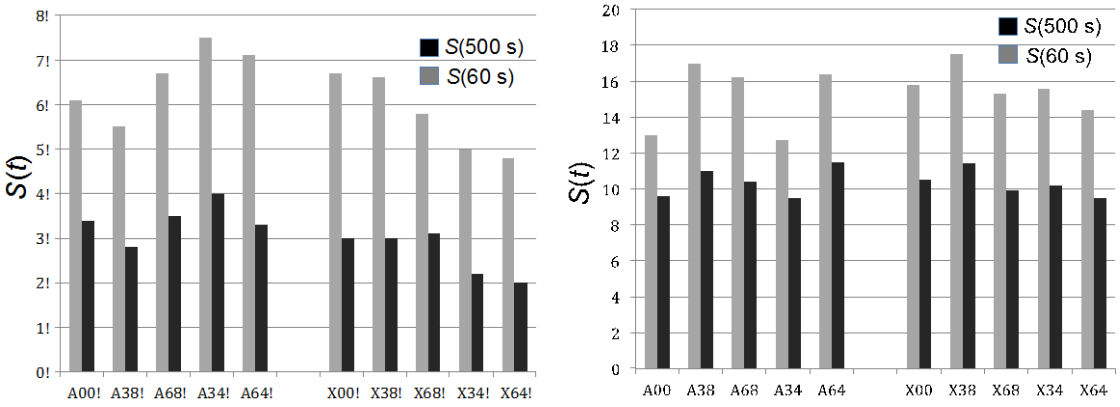

(a) (b)

FIGURE 5.1: creep stiffness $S(t)$ (GPa) of mix design group 1 at (a) T = −18°C and (b) T = −28°C.

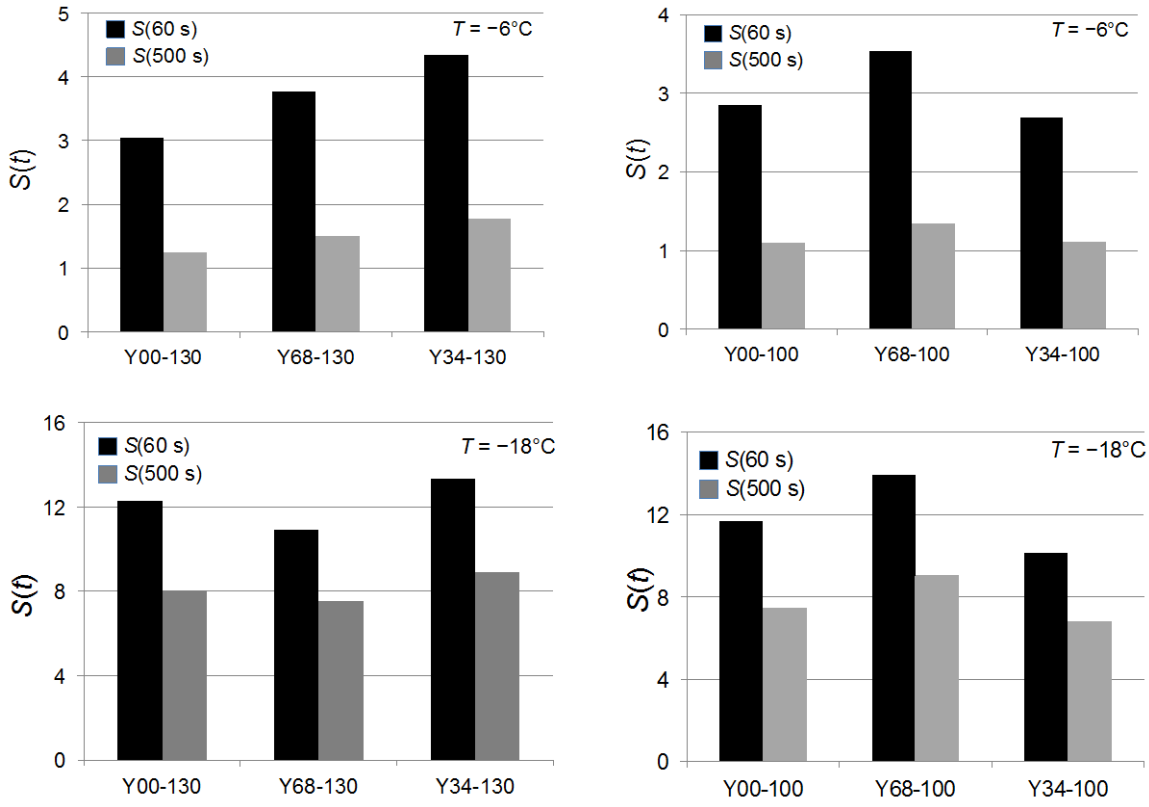

FIGURE 5.2: creep stiffness $S(t)$ (GPa) of mix design group 2 at (a) T = −18°C and (b) T = −28°C.

Based on Figure 5.2, it can be seen that at T = −6°C and for mixtures compacted at 130°C the addition of GNPs consistently leads to an increase in creep stiffness S(60 s) and S(500 s). The increase could be as high as 30%. However, for mixtures compacted at 100°C, the creep stiffness measured at T = −6°C is found to vary between −6% and +24%. This indicates that, even with the same final air void content, the compaction temperature could influence how the GNPs affect the creep stiffness. At T = −18°C, both mixtures compacted at 100°C and 130°C do not show a monotonic increase or decrease in creep stiffness. For mixtures compacted at 130°C the addition of GNPs leads to a variation between −10% and +12%, and for mixtures compacted at 100°C the variation is between −10% and +20%. Furthermore, it is interesting to observe that for mixture compacted at 100°C, the GNPs have almost the same effect on the creep stiffness measured at T = −6°C and −18°C. For instance, the addition of 6% of GNP M850 always leads to an increase in creep stiffness and 3% 4827 results in a decrease. However, the opposite trend is seen for the creep stiffness measured at T = −18°C of mixtures compacted at 130°C, which further demonstrates the significant influence of the compaction temperature on the creep stiffness of the GNP-reinforced asphalt mixtures.

5.3 IDT STRENGTH TEST

Based on the same standard test method, strength properties were investigated. For mix design group 1, the IDT strength tests were performed at T = −18°C and −28°C, and for the mix design group, the tests were performed at T = −6°C because of the limited number of available specimens. For each mix, three replicates were tested and the average results were used for the analysis, as shown in Figure 5.3.

For mix design group 1, it is clear that the addition of GNPs in the mixtures with the polymer-modified binder leads to an increase in IDT strength at both testing temperatures. The biggest increase, 13% for both temperatures, is observed for the A68 mixture; that is, the addition of 6% GNP M850. For mixtures with the unmodified binder a smaller increase, up to 11%, was observed. The maximum averaged increase at these two temperatures was seen in the case of the addition of 3% GNP M850. It is interesting to note that the increase in IDT strength of GNP-reinforced mixture specimens is much less pronounced than that of GNP-reinforced binder specimens. One possible explanation for this observation is that a considerable amount of damage may occur along the interface between the binder and aggregate. However, direct addition of GNP materials into the asphalt binder may not effectively enhance the interfacial strength, which leads to a less significant increase in IDT strength.

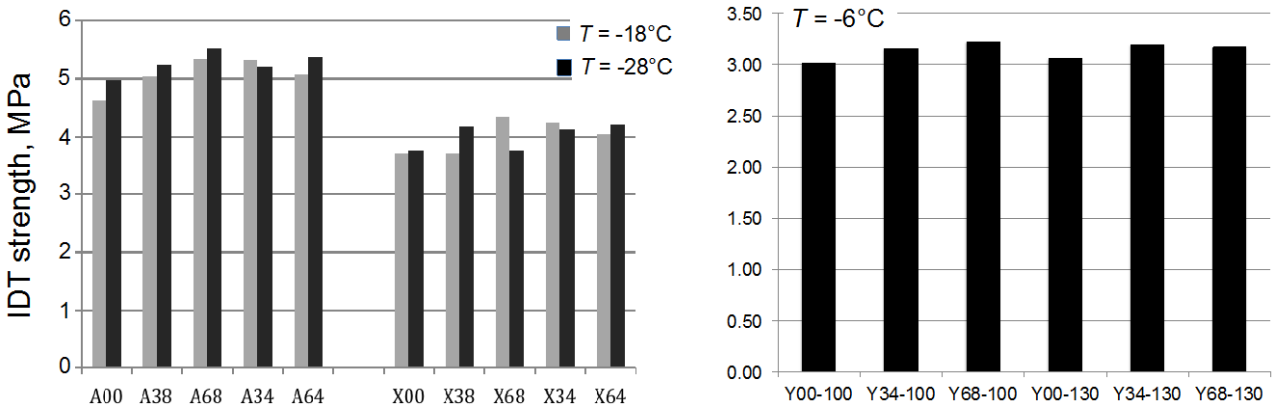

FIGURE 5.3: Results of IDT strength of GNP-reinforced asphalt mixtures.

For mix design group 2, the increase in IDT strength is less pronounced than that of mix design group 1. Meanwhile, it can also be observed that the compaction temperature does not have a significant effect on the strength improvement of GNP-reinforced asphalt mixtures. This observation could also be explained by the fact that the aggregate-binder may not effectively be strengthened by the GNPs. Therefore, the compaction temperature is expected to have a small effect on the strength property since all specimens are compacted to the same air void content.

5.4 FRACTURE ENERGY TEST

To measure the fracture energy, which is the energy required to propagate a macroscopic crack by a unit length, we performed the SCB test following AASHTO TP-105 (*39*). The fracture energy measured by the SCB test is a material property that represents the fracture resistance under mode-I loading (tensile fracture). The SCB test method takes

advantage of the simple specimen preparation from Superpave Gyratory compacted cylinders and the simple loading setup (*40*). Figure 5.4 shows the set-up of SCB tests.

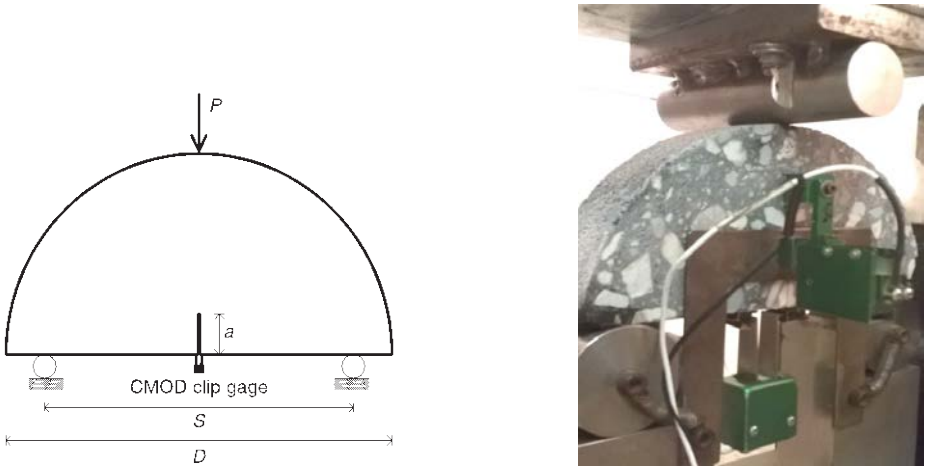

FIGURE 5.4: Set-up of SCB tests.

In this research, a MTS servo-hydraulic testing system equipped with an environmental chamber was used to perform the SCB test. The SCB samples were symmetrically supported by two fixed rollers and had a span of 120 mm. The load line displacement (LLD) was measured using a vertically mounted Epsilon extensometer with a 38-mm gage length and ±1 mm range; one end was mounted on a button that was permanently fixed on a specially made frame and the other end was attached to a metal button glued to the sample. The CMOD was recorded by an Epsilon clip gage with a 10-mm gage length and a +2.5 and −1 mm range. The clip gage was attached at the bottom of the specimen. Considering the brittle behavior of asphalt mixtures at low temperatures, the CMOD signal was used as the control signal to maintain the test stability in the post-peak region of the test. A constant CMOD rate of 0.0005mm/s was used and the load and load-point displacement (*P*-*u*) curve was plotted. A contact load with maximum load magnitude of 0.3 kN was applied before the actual loading to ensure uniform contact between the loading plate and the specimen. The testing was stopped when the load dropped to 0.5 kN in the post-peak region. All tests were performed inside an environmental chamber. Liquid nitrogen was used to obtain the required low temperature. The temperature was controlled by the environmental chamber temperature controller and verified using an independent platinum RTD thermometer. For mix design group 1, the SCB tests were performed at $T = -24$°C, and the SCB tests on mix design group 2 were performed at $T = -18$°C. Similar to the aforementioned IDT creep and strength tests, three replicates were tested for each mix.

The fracture energy G_f was calculated according to RILEM TC 50-FMC specification that has been extensively used in the study of concrete. The work of fracture is determined as the area under the loading-deflection (*P*-*u*) curve. The fracture energy G_f can then be obtained by dividing the work of fracture with the ligament area:

$$G_f = \frac{\int P\,\mathrm{d}u}{A_l} \tag{5.1}$$

where: $\int P\,\mathrm{d}u$ =total work done by the external force *P*, and A_l = ligament area. Eq. 5.1 is based on the assumption that the external work is all spent in crack propagation and the rest part of the specimen behaves elastically. This assumption is reasonable for asphalt mixture specimens at low temperatures, which generally exhibit a damage localization mechanism (*39, 41*). One difficulty using this approach is that it is next to impossible to capture the tail part of the load-deflection curve. This is because, as the crack propagates close to the top surface of the specimen, the CMOD opening typically exceeds the allowable gauge measurement limit and the test is terminated. Therefore, in this study we use some polynomials to fit the measured post-peak region of the *P*-*u* curve and perform an analytical integration to obtain the external work done by the force *P*. Figure 5.5 shows a typical example of measured *P*-*u* curves.

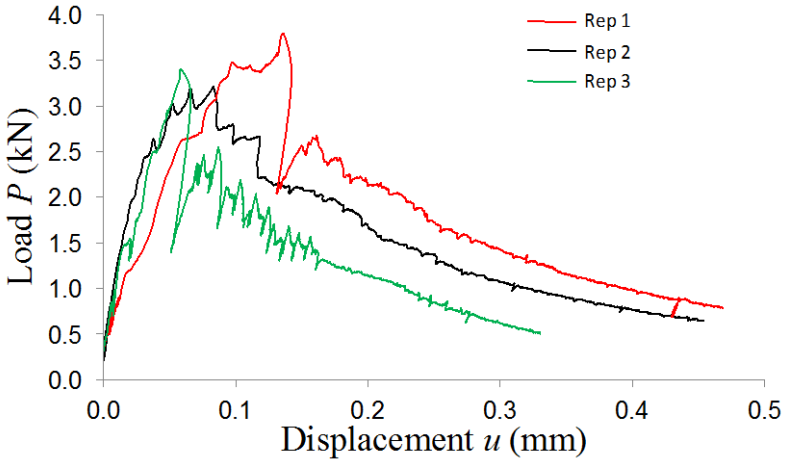

FIGURE 5.5: Measured load-displacement curves of three SCB specimens.

It can be noted that the apparent fracture toughness can also be calculated from the measured peak load of the specimen within the framework of linear elastic fracture mechanics (LEFM). The essential failure criterion of LEFM is that the stress intensity factor (SIF) of the specimen reaches a critical value (i.e., fracture toughness) as the peak load is attained. Considering the LEFM failure criterion, we can compute that the fracture toughness K_{1c} is based on the experimentally measured peak load. It should be noted that the computed fracture toughness is strictly anchored by the assumption of LEFM. For SCB specimens, it has been found that the LFEM limit may not be achieved since the fracture process zone at the crack tip is not necessarily negligible compared with the specimen size (*41–43*). Therefore, we refer this calculated K_{1c} as to the apparent fracture toughness, which would strongly depend on specimen geometry and size, and it does not directly measure the fracture resistance of the material. Therefore in this study we choose to use the fracture energy as a measure of fracture resistance.

Figure 5.6 presents the average values of the fracture energy, G_f, of both mix design groups 1 and 2. Based on the results of the mix design group 1, it can be observed that for mixtures with the polymer-modified binder the addition of GNPs leads to a considerable increase (about 28%) in fracture energy. For example, addition of GNP M850 with 6% by weight of binders gives rise to almost 100% increase in fracture energy. For unmodified binder asphalt mixtures, the results are mixed. It is seen that the addition of GNP M850 and GNP 4827 generally causes a decrease in fracture energy, except GNP 4827 where 3% addition is beneficial. The present experiments indicate that the effect of GNP addition on the fracture energy for mixtures with the modified binder is opposite to that for mixtures with the unmodified binder.

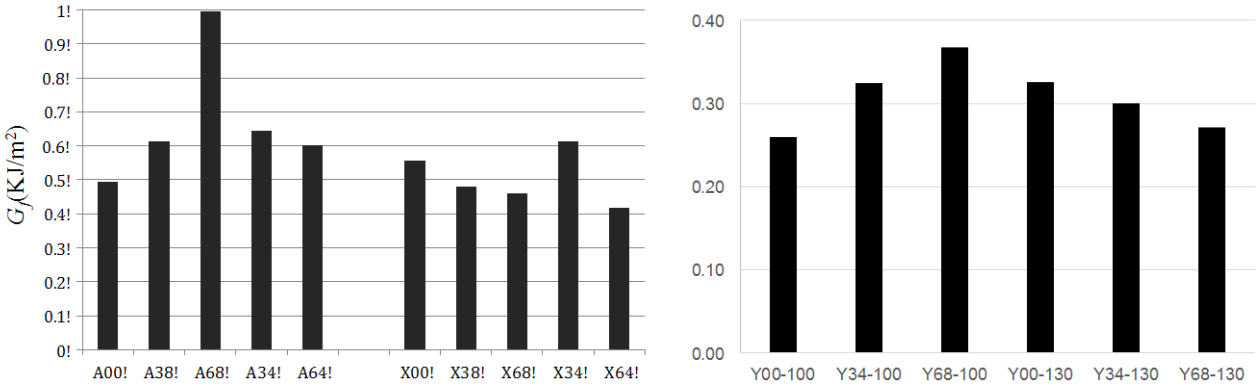

FIGURE 5.6: Fracture energy of GNP-reinforced asphalt mixtures.

For mix design group 2, it has been found that for mixtures compacted at 100°C the addition of GNPs leads to a consistent increase in fracture energy as high as 41%. By contrast, the GNPs result in a decrease in fracture energy of mixtures compacted at 130°C, which is similar to the trend observed in unmodified binder of the mix design group 1. This observation indicates that the effect of GNP on fracture energy of the mixture is influenced by the compaction temperature. This is different from the observed compaction temperature effect on the IDT strength. This is because the

IDT strength is governed by one failure location as the load capacity is reached. By contrast, the fracture energy is calculated by considering the entire failure path of the specimen, which contains both the binder and the binder–aggregate interface. Therefore, we observe a stronger influence of the compaction temperature on the fracture energy of GNP-reinforced asphalt mixtures. It can also be noted that in the present experiments all the specimens are compacted at the same target air void content. If the compaction were done at the same number of gyrations, the GNP-reinforced asphalt mixtures would have a lower air void content, which could lead to a considerable improvement of the fracture properties.

So far it is still unclear why there is a decrease in fracture energy at a higher dose of GNP addition for these particular mix designs. Further investigation would be needed, in which a smaller dose of GNP should be considered to confirm such a trend. Meanwhile, it would also be important to study the adhesive and cohesive properties of GNP-reinforced binders and mixtures to gain a better understanding of the effect of GNPs on the fracture energy of asphalt mixtures.

5.5 CONCLUSIONS

The results of the present investigation of GNP-reinforced asphalt mixtures can be summarized as follows:

1. The addition of GNPs could lead to an increase or a decrease in creep stiffness of asphalt mixtures, depending on the mix design. The test results also indicate that the effect of GNPs on the creep stiffness is strongly influenced by the compaction temperature as well as the temperature at which the creep stiffness is measured.
2. The addition of GNPs results in a moderate improvement in IDT strength. This improvement is much less pronounced than that for GNP-reinforced binders. One possible reason for such a difference is that for GNP-reinforced asphalt mixtures the failure location at the peak load is likely along the aggregate–binder interface, which may not effectively be enhanced by the GNPs. Due to the same reason, it is found that the compaction temperature does not have a significant effect on the IDT strength of GNP-reinforced asphalt mixtures.
3. The SCB tests show that the addition of GNPs could cause an increase in fracture energy of asphalt mixtures in which the SBS-modified binders are used. For mixtures with unmodified binders tested in this study, the GNPs could also improve the fracture energy for the case where the mixtures are compacted at a low temperature, whereas for mixtures compacted at a higher temperature the GNPs are found to lead to a decrease in fracture energy.

CHAPTER 6

INVESTIGATION OF ELECTRICAL CONDUCTIVITY

This chapter investigates the electrical conductivity of GNP-reinforced asphalt binders, which is motivated by the potential use of the electrical conductivity property for damage sensing (*28*). The investigation involves two different types of binders with the addition of two types of GNPs. The electrical conductivity is measured through a 4-probe method. The test result is discussed in the framework of the percolation theory.

6.1 SAMPLE PREPARATION

This investigation focuses on GNP-reinforced asphalt binders, in which four different ways were used to prepare the beam specimens. The test materials are listed in Table 6.1.

TABLE 6.1 Sample descriptions

Sample Preparation Method	Binder type	Percent and Type of GNP Materials				
		0%	1.5%	3%	6%	10%
A	PG 52-34	—	M850 4827	M850 4827	M850 4827	M850 4827
A	PG 64-34	—	M850 4827	M850 4827	M850 4827	M850 4827
B	PG 52-34	—		M850 4827	M850 4827	
B	PG 64-34	—		M850 4827	M850 4827	
C	PG 52-34	X		M850 4827	M850 4827	
C	PG 64-34	X		M850 4827	M850 4827	
D	Emulsion	X		M850 4827	M850 4827	

The detailed preparation methods are described as follows:

A. The binder and the GNPs were heated at 150°C. The GNPs were added to the binder while the binder can was seated on a hot plate and the mix was stirred by hand for 15 minutes. After that, the mix was poured into the mold for 1 hour. After demolding, the beams were stored in the fridge.
B. The binder and the GNPs were heated at 150°C. A pan containing 10 lb of sand was also heated at 150°C and then placed on a vibrating flat lap. The small can, which contains the binder and the GNP, was covered with hot sand in the pan and kept for 30 minutes on the vibrating flat lap. After that, the mix was reheated and poured into the mold for 1 hour. After demolding, the beams were stored in the fridge.
C. The binder and the GNPs were heated at 150°C. The GNPs were added to the binder and stirred for 15 minutes using a paint mixer. The mix was then reheated and poured into the mold for 1 hour. After demolding, the beams were stored in the fridge.
D. The emulsion (Co AE13-343), with a distillation residue of 61% and a weight/gallon of 8.465 lb, was mixed at room temperature with the GNP by hand. Then it was cured using two methods:
    - The RTFO method: the binder–GNP mix was kept in the RTFO first for 15 minutes at 85°C and then for another 20 minutes at 145°C
    - Air drying for 24 hours in a PAV pan at room temperature and then for 2 hours at 60°C in an oven.

An aluminum mold was used to prepare a 5-in. long, ½-in. tall, and ¼-in.thick beam sample. Four electrodes made from aluminum screening (mesh) were seated into the mold (Figure 6.1a) and the distance between them was kept constant during the sample preparation. After curing, the mix was reheated and poured into these molds after 1 hour. The demolded beams were stored in the fridge. Figure 6.1b shows the test specimen.

(a) (b)

FIGURE 6.1: (a) mold preparation (b) beam cured with four electrodes.

6.2 TEST METHOD AND RESULTS

In this study, the standard 4-probe measurement was used shown as Figure 6.2. A power source type Keithley 2401 Source meter and a FLUKE multimeter were used for testing. A constant direct current was applied to the outer two electrodes using the power source. The multimeter was used to measure the potential difference between the two inner electrodes. The values used for the DC current were 0.01 mA, 0.1 mA, 1 mA, and 10 mA. In this experiment, the multimeter did not measure a potential difference in any of these cases, which indicates that no current was passing through the beam. Among all specimens tested, it is interesting to note that for the fresh made emulsion beams a small amount of current was measured at the uncured stage, and after the beams were cured for 72 hours in air at room temperature, no potential difference was measured between the electrodes.

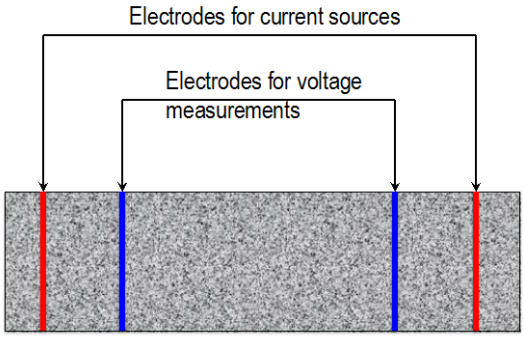

FIGURE 6.2: Schematics of 4-probe measurement of electrical conductivity.

It is worthwhile to comment on the failure of improvement of the electrical conductivity of GNP-reinforced asphalt binders. The basic mechanism for enhancing the electrical conductivity through GNP addition is that the GNPs can be dispersed to the extent that the spacing between them is small enough for the electrons to hop. This mechanism can be analyzed by the percolation theory. Li and Kim (*26*) recently derived an analytical expression on the percolation threshold of nanocomposites containing 3D random-distributed disc-shaped nanoparticles based on the average interparticle distance approach:

$$V_{tr} = \frac{27\pi d^2 t}{4(d + s_{ip})^3} \tag{6.1}$$

where V_{tr} is the threshold of volume ratio of the binders, d = diameter of the GNP disk, t = thickness of the GNP disk, s_{ip} is the maximum spacing that allows for electron hopping to take place between adjacent conductive fillers owing to quantum-mechanical tunneling. The s_{ip} is expected to be on the order of 10 nm. For GNP, Eq. 6.1 gives $V_{tr} \approx 2.4\%$. Based on the density of binder and GNPs, the volume ratio corresponds to a mass ratio of 4%–5%. This was the basis for

choosing 3% and 6% mass ratio for the aforementioned mechanical tests. Based on the calculation of Eq. 6.1, it is clear that the 1.5% and 3% addition of GNPs will not lead to an improvement of electrical conductivity.

Meanwhile, it should also be pointed out that Eq. 6.1 was derived based on the assumption that the nanoparticles are uniformly distributed in space and size, which was unlikely to be achieved in GNP-reinforced asphalt binders. Therefore, the actual percolation threshold could be much higher than the prediction by Eq. 6.1. On the other hand, after increasing the GNP to 10%, the mix could not be poured into the mold at a temperature lower than 180°C. Raising the temperature above 160°C may affect the binder properties and for this reason the percent of GNP in binder by weight was limited to 6%. This practical difficulty of mixing limits the maximum amount of GNPs that can be added to the binders. In this regard, a better mixing procedure is needed for improving the electrical conductivity for a limited amount of GNP dose.

The present study on the uncured emulsion beams indicates that the electrical conduction can be achieved if there is some amount of water present in the materials. We may expect that, even with the aforementioned three different mixing methods, the GNP particles cannot be dispersed in the binders to the extent that allows the electrons to hop between them and therefore it would need to rely on water to assist the electrical conduction. Once the water is evaporated, the GNP particles themselves are not able to transport the electrons. It should be mentioned here that the water itself is insufficient to make the material conductive because the water present in the material does not necessarily form a continuous medium to transport the electrons. Therefore, it is both water and GNP that makes the uncured emulsion beams electrically conductive.

6.3 CONCLUSIONS

The present investigation shows that with the currently used mixing procedure the GNP-reinforced asphalt binders are generally not electrically conductive. With the percolation theory, this experimental observation indicates that the dispersion of GNPs in binders cannot reach a homogenous state. This could be because the GNPs are directly mixed with viscous binders, where the mixing is not sufficiently effective to create a network for electron hopping even though the amount of GNP addition is beyond the theoretical threshold. Meanwhile, it is noted that if there is some amount of water present in the binders, the addition of GNPs could make the material electrically conductive with a high electrical resistance. Therefore, we can conclude that in general the GNP-reinforced asphalt binders and mixtures cannot likely be used as a damage sensing material through the measurement of electrical resistance.

CHAPTER 7

CONCLUSIONS, PLANS FOR IMPLEMENTATION, AND RECOMMENDATIONS FOR FURTHER RESEARCH

7.1. CONCLUSIONS

This project develops graphene nanoplatelet (GNP) reinforced asphalt binders and mixtures and investigates their mechanical properties. This represents the first step of exploring the potential applications of this new type of materials for asphalt pavements. GNP materials are made from graphene, which is known for its excellent mechanical and electrical properties. The cost of GNPs is significantly lower than other types of graphene-based materials, which makes GNPs ideal for large-scale applications. Meanwhile, compared with the conventional carbon nanotubes, the GNPs have a low aspect ratio, which makes them easier to disperse. This opens up many opportunities for the application of GNPs in asphalt pavements.

The investigation of GNP-reinforced asphalt binders shows that for both conventional polymer-modified and unmodified asphalt binders the addition of GNPs does not have a significant effect on the complex modulus of the binder. Experiments also show that the addition of GNPs does not significantly affect the relaxation properties of the binder. On the contrary, it is observed that the incorporation of GNPs into binders leads to a remarkable improvement in the flexural strength at low temperatures. For both polymer-modified and unmodified asphalt binders a moderate addition of GNPs; that is, 3% to 6% by weight of the binder, could result in a 130% increase in flexural strength. It should be noted that such an increase has never been seen in polymer-modified asphalt binders. On the other hand, it is found that the strength improvement becomes less pronounced when a large amount of GNP addition is used. This could be caused by potential clumping of GNPs at a large dose.

The compaction experiments of GNP-reinforced asphalt mixtures indicate that the GNP-reinforced binders can significantly improve the compaction performance of the mixtures. The GNPs could lead to a 20%–40% reduction in the number of compaction gyrations to achieve a prescribed target air void content. It is also found that for some mix designs the GNPs could also reduce the temperature dependence of the compaction gyration. This would allow engineers to produce warm asphalt mixtures. The test results indicate that for a given number of compaction gyrations the addition of GNPs could effectively reduce the air void content of the asphalt mixtures, which would improve the long-term durability of the pavements. In parallel with the compaction tests, a set of rut experiments is performed and it is demonstrated that the addition of GNP could improve the rut performance of the pavements at intermediate temperatures. Nevertheless, it can be observed that the addition of GNPs could adversely affect the rut performance if the mixtures are compacted at a lower temperature.

The experiments on the mechanical properties of GNP-reinforced asphalt mixtures indicate that depending on the mix design and the compaction temperature the GNP could result in either an increase or a decrease in creep stiffness. The addition of GNPs would lead to a moderate increase in IDT strength. Compared with the increase in flexural strength of GNP-reinforced asphalt binders this increase is much less. This could be attributed to that considerable amount of damage that could occur at the interface between the binder and aggregates, which may not be effectively reinforced by the GNP materials. On the other hand, the GNP does not necessarily improve the fracture energy. The present studies show that for mixtures with modified binders the GNP would enhance the fracture energy, and the same trend is observed for mixtures with unmodified binders compacted at a lower temperature. However, for mixtures with unmodified binders compacted at a higher temperature, the GNP is found to have an adverse effect on the fracture energy.

The electrical resistance experiment shows that with the current mixing procedure the GNPs generally would not make the binders electrically conductive. This could be because the dispersion of GNPs in binders cannot reach a homogenous state for the generating network for electron hopping even though the amount of GNP addition is beyond the theoretical percolation threshold. Meanwhile, it can be found that, if there is some amount of water present in the binders, the addition of GNPs could make the material electrically conductive with a high electrical resistance.

In summary, the results of this research indicate that the addition of GNPs could improve a number of mechanical and compaction properties and therefore enhance the performance of the asphalt pavements. With a relatively low material cost, the GNP-reinforced asphalt binders and mixtures have a potential for large-scale applications in the pavement industry, which includes both new pavement construction and pavement rehabilitation.

7.2. PLANS FOR IMPLEMENTATION

This research was presented at national and international meetings and has received considerable attention over the past year. Minnesota Department of Transportation (MnDOT) has expressed a strong interest in further investigating this type of new materials for field applications. A research project has recently been awarded by MnDOT to explore the use of GNP-reinforced asphalt binders and mixtures for pothole repair. A U.S. patent (pending) has been filed for this type of new materials. The PI plans to promote these new materials to the pavement industry through MnDOT and the University of Minnesota Technology Commercialization Office.

7.3. RECOMMENDATIONS FOR FURTHER RESEARCH

The results obtained in this investigation show some promising properties of GNP-reinforced asphalt binders and mixtures, which could potentially be used as a new type of pavement materials. Several important issues need to be further addressed:

1. The current research is limited to laboratory testing and the number of test specimens is rather small, which leads to the conclusion that some test results are subjected to a considerable scattering. For full implementation of these materials, more extensive laboratory experiments will be needed to achieve more consistent results with statistical information. In addition to laboratory tests, it is also necessary to perform field experiments on the construction of GNP-reinforced asphalt pavements as well as the performance of these pavements subjected to different types of loads and weather conditions. A cost-benefit analysis will also be needed to evaluate the financial gain for using the GNP-reinforced asphalt pavements.
2. The present experiments indicate that the strength improvement of GNP-reinforced asphalt binders is significantly larger than that of GNP-reinforced asphalt mixtures. Further effort is needed to investigate the mechanisms responsible for this phenomenon and to explore new ways of mixing GNP with the binders and aggregates to further enhance the improvements of the properties of GNP-reinforced asphalt mixtures.
3. The SCB experiments show that, for the particular mix designs considered in this study, the GNP could have an adverse effect on the fracture energy of mixtures, which is counter-intuitive since the GNP has excellent mechanical properties. Further investigation is needed to study the cohesion of GNP-reinforced binders, the adhesive between the GNP-reinforced binders and the aggregate, as well as the chemistry between the GNP and asphalt binders, which will allow us to improve the mix design.
4. It will also be desirable to investigate other properties of GNP-reinforced asphalt mixtures, such as the moisture susceptibility, impacts on mixes with polyphosphoric acid binders, re-refined engine oil bottom, lime, and anti-strips. In addition, fatigue cracking resistance and block cracking by using the new SCB test methods proposed for intermediate temperature should also be investigated for GNP-reinforced asphalt mixtures.

REFERENCES

1. Steyn, W.J., "Applications of Nanotechnology in Road Pavement Engineering," *Nanotechnology in Civil Infrastructure*, 2011, pp. 49–83.
2. Shirakawa, T., A. Tada, and N. Okazaki, "Development of Functional Carbon Nanotubes–Asphalt Composites," *International Journal of GEOMATE*, Vol. 2, No. 1, 2012, pp. 161–165.
3. Novoselov, K.S., A.K. Geim, S.V. Morozov, D. Jiang, M.I. Katsnelson, I.V. Grigorieva, S.V. Dubonos, and A.A. Firsov, "Two-Dimensional Gas of Massless Dirac Fermions in Graphene," *Nature*, Vol. 438, 2005, p. 197.
4. Zhang, Y., Y.W. Tan, H.L. Stormer, and P. Kim, "Experimental Observation of the Quantum Hall Effect and Berry's Phase in Graphene," *Nature*, Vol. 438, 2005, p. 201.
5. Lee, C., X. Wei, J.W. Kysar, and J. Hone, "Measurement of the Elastic Properties and Intrinsic Strength of Monolayer Graphene," *Science*, Vol. 321, 2008, p. 385.
6. Kim, K., W. Regan, B. Geng, B. Aleman, B.M. Kessler, F. Wang, M.F. Crommie, and A. Zettl, "High-Temperature Stability of Suspended Single-Layer Graphene," *Physica Status Solidi*, RRL4, No. 11, 2010, pp. 302–304.
7. Berman, D., A. Erdemir, and A.V. Sumant, "Graphene: A New Emerging Lubricant," *Materials Today*, Vol. 17, No. 1, 2014, pp. 31–42.
8. Yang, J. and S. Tighe, "A Review of Advances of Nanotechnology in Asphalt Mixtures," *Procedia—Social and Behavioral Sciences*, 2013, pp. 1269–1276.
9. Nanoclays. (n.d.)[Online]. Available: http://www.sigmaaldrich.com/materials-science/nanomaterials/nanoclay-building.html [accessed July 31, 2915].
10. Yao, H., L. Li, H. Xie, H. Dan, and X. Yang, "Microstructure and Performance Analysis of Nanomaterials Modified Asphalt," *Road Materials and New Innovations in Pavement Engineering*, 2011, pp. 220–228.
11. Hossain, Z., M. Zaman, M. Saha, and T. Hawa, "Evaluation of Viscosity and Rutting Properties of Nanoclay-Modified Asphalt Binders," *Geo-Congress 2014*, 2014, pp. 3695–3702.
12. Jahromi, S. and K.A. Ghaffarpour, "Effects of Nanoclay on Rheological Properties of Bitumen Binder," *Construction and Building Materials*, Vol. 23, 2009, pp. 2894–2904.
13. Zare-Shahabadi, A., A. Shokuhfar and S. Ebrahimi-Nejad, "Preparation and Rheological Characterization of Asphalt Binders Reinforced with Layered Silicate Nanoparticles," *Construction and Building Materials*, Vol. 24, No. 7) 2010, pp. 1239–1244.
14. Nazzal, M., S. Kaya, T. Gunay, and P. Ahmedzade, "Fundamental Characterization of Asphalt Clay Nanocomposites," *Journal of Nanomechanics and Micromechanics*, Vol. 3, No. 1, 2013, pp. 1–8.
15. Abdelrahman, M., D. Katti, A. Ghavibazoo, H. Upadhyay, and K. Katti," "Engineering Physical Properties of Asphalt Binders Through Nanoclay–Asphalt Interactions," *Journal of Materials in Civil Engineering*, Vol. 26, No. 12, 2014.
16. Mun, S. and H. Lee, "Modeling Viscoelastic Crack Growth in Hot-Mix Asphalt Concrete Mixtures Using a Disk-Shaped Compact Tension Test," *Journal of Engineering Mechanics*, Vol. 137, No. 6, 2011, pp. 431–438.
17. Barik, T.K., B. Sahu, and V. Swain, "Nanosilica-from Medicine to Pest Control," *Parasitology Research*, Vol. 103, 2008, pp. 253–258.
18. Yao, H., Z. You, L. Li, C. Lee, D. Wingard, Y. Yap, X. Shi, and S. Goh, "Rheological Properties and Chemical Bonding of Asphalt Modified with Nanosilica," *Journal of Materials in Civil Engineering*, Vol. 25, No. 11, 2013, pp. 1619–1630.
19. Yan, Y., C. Cocconcelli, R. Roque, T. Nash, J. Zou, D. Hernando, and G. Lopp, "Performance Evaluation of Alternative Polymer-Modified Asphalt Binders," *Road Materials and Pavement Design*, Vol. 16, 2015, pp. 389–403.
20. Yusoff, N., A. Breem, H. Alattug, A. Hamim, and J. Ahmad, "The Effects of Moisture Susceptibility and Ageing Conditions on Nano-Silica/Polymer-Modified Asphalt Mixtures," *Construction and Building Materials*, Vol. 72, 2014, pp. 139–147.
21. Al-Adham, K. and M. Arifuzzaman, "Moisture Damage Evaluation in Carbon Nanotubes Reinforced Asphalts," In *Sustainability, Eco-efficiency, and Conservation in Transportation Infrastructure Asset Management*, 2014, pp. 103–109.
22. Arabani, M. and M. Faramarzi, "Characterization of CNTs-Modified HMA's Mechanical Properties," *Construction and Building Materials*, Vol. 83, 2015, pp. 207–215.
23. *Basalt Fiber Properties, Advantages and Disadvantages*, n.d. [Online]. Available: http://www.build-on-prince.com/basalt-fiber.html#sthash.1bkllF7E.dpbs [accessed July 31, 2015].
24. Gu, X., T. Xu and F. Ni, "Rheological Behavior of Basalt Fiber Reinforced Asphalt Mastic," *Journal of Wuhan University of Technology-Material Science Edition*, Vol. 29, No. 5 2014, pp. 950–955.

25. Zheng, Y., Y. Cai, G. Zhang, and H. Fang, "Fatigue Property of Basalt Fiber-Modified Asphalt Mixture Under Complicated Environment," *Journal of Wuhan University of Technology—Material Science Edition*, Vol. 29, No. 5, 2014, pp. 996–1004.
26. Wang, D., L. Wang, X. Gu, and G. Zhou, "Effect of Basalt Fiber on the Asphalt Binder and Mastic at Low Temperature," *Journal of Materials in Civil Engineering*, Vol. 25, No. 3, 2013, pp. 355–364.
27. Gao, C., S. Han, S. Chen, and H. Li, "Research on Basalt Fiber Asphalt Concrete's Low Temperature Performance," *AMM Applied Mechanics and Materials*, Vols. 505–506, 2014, pp. 35–38.
28. Le, J.-L., H. Du, and S. D. Pang, "Use of 2D Graphene Nanoplatelets (GNP) in Cement Composites for Structural Health Evaluation," *Composites Part B: Engineering*, Vol. 67, pp. 555–563.
29. Du, H. and S.D. Pang, "Enhancement of Barrier Properties of Cement Mortar with Graphene Nanoplatelet," *Cement and Concrete Research*, Vol. 76, 2015, pp. 10–19.
30. Du, H. and S.D. Pang, "Mechanical Response and Strain Sensing of Cement Composites Added with Graphene Nanoplatelet Under Tension," In *Nanotechnology in Construction*, 2015, pp. 377–382.
31. American Association of State Highway and Transportation Officials (AASHTO), AASHTO T240-09-UL, Test for effect of heat and air on a moving film of asphalt (Rolling Thin-Film Oven Test), AASHTO, Washington, D.C., 2009.
32. American Association of State Highway and Transportation Officials (AASHTO), AASHTO R028-09-UL, Standard Practice for Accelerated Aging of Asphalt Binder Using a Pressurized Aging Vessel (PAV), AASHTO, Washington, D.C., 2009.
33. American Association of State Highway and Transportation Officials (AASHTO), AASHTO T315-12-UL, Standard Method of Test for Determining the Rheological Properties of Asphalt Binder Using a Dynamic Shear Rheometer (DSR), AASHTO, Washington, D.C., 2012.
34. American Association of State Highway and Transportation Officials (AASHTO), AASHTO T313-10-UL, Determining the Flexural Creep Stiffness of Asphalt Binder Using the Bending Beam Rheometer (BBR), AASHTO, Washington, D.C., 2010.
35. Konsta-Gdoutos, M.S., Z.S. Metaxa, and S.P. Shah, "Highly Dispersed Carbon Nanotube Reinforced Cement Based Materials," *Cement and Concrete Research*, Vol. 40, 2010, pp. 1052–1059.
36. American Association of State Highway and Transportation Officials (AASHTO), AASHTO T166-10-UL, Standard Method of Test for Bulk Specific Gravity of Compacted Hot Mix Asphalt (HMA) Using Saturated Surface-Dry Specimen, AASHTO, Washington, D.C., 2010.
37. American Association of State Highway and Transportation Officials (AASHTO), AASHTO T209-10-UL, Standard Method of Test for Theoretical Maximum Specific Gravity and Density of Hot Mix Asphalt (HMA), AASHTO, Washington, D.C., 2010.
38. American Association of State Highway and Transportation Officials (AASHTO), AASHTO T322-07, Standard Method of Test for Determining the Creep Compliance and Strength of Hot-Mix Asphalt (HMA) Using the Indirect Tensile Test Device, AASHTO, Washington, D.C., 2007.
39. American Association of State Highway and Transportation Officials (AASHTO), AASHTO TP 105-2013 Standard Method of Test for Determining the Fracture Energy of Asphalt Mixtures Using the Semicircular Bend Geometry (SCB), AASHTO, Washington, D.C., 2013.
40. Marasteanu, M.O., A. Zofka, M. Turos, X. Li, R. Velasquez, X. Li, W. Buttlar, G. Paulino, A. Braham, E. Dave, J. Ojo, H. Bahia, C.J. Bausano, A. Gallistel, and J. McGraw, Investigation of Low Temperature Cracking in Asphalt Pavements: National Pooled Fund Study 776. Final Report, Minnesota Department of Transportation, St. Paul, 2007.
41. Le, J.-L., A. Cannone Falchetto, and M.O. Marasteanu, "Determination of Strength Distribution of Quasibrittle Structures from Size Effect Analysis," *Mechanics of Materials*, Vol. 66, 2013, pp. 79–87.
42. Zegeye, E., J.-L. Le, M. Turos, and M.O. Marasteanu, "Investigation of Size Effect in Asphalt Mixture Fracture Testing at Low Temperature," *Road Materials and Pavement Design*, Vol. 13, 2012, S1, pp. 88–101.
43. Cannone Falchetto, A., J.-L. Le, M.I. Turos and M.O. Marasteanu, "Indirect Determination of Size Effect on Strength of Asphalt Mixtures at Low Temperatures," *Materials and Structures*, Vol. 47, 102, 2014, 157–169.